ELSEVIER

J. Non-Newtonian Fluid Mech. xxx (2007) xxx–xxx

Journal of Non-Newtonian Fluid Mechanics

www.elsevier.com/locate/jnnfm

Instability of coextruded elastic liquids at high Weissenberg number

Joel C. Miller [a,b,*,1], J.M. Rallison [a]

[a] *Department of Applied Mathematics and Theoretical Physics, University of Cambridge, Cambridge CB3 0WA, UK*
[b] *Mathematical Modeling & Analysis Group and Center for Nonlinear Studies, MS B284, Los Alamos National Laboratory, Los Alamos, NM 87545, USA*

Received 7 July 2006; received in revised form 11 January 2007; accepted 23 January 2007

Abstract

We reconsider the linear stability of pressure-driven flow of two Oldroyd-B or UCM fluids symmetrically placed in a channel or a pipe (a "coextrusion flow"). The fluids have matched viscosities but different relaxation times. Inertia and surface tension are neglected. We focus on the high Weissenberg number limit, where the distance travelled by a fluid particle in a relaxation time is large compared to the width of the channel. Given a prescribed location of the unperturbed interface, the growth rate at sufficiently high wavenumber can be deduced from previous analysis of Couette flow [Y. Renardy, Stability of the interface in two-layer Couette flow of upper convected Maxwell liquids, J. Non-Newtonian Fluid Mech. 28 (1988) 99–115; K. Chen, D.D. Joseph, Elastic short-wave instability in extrusion flows of viscoelastic liquids, J. Non-Newtonian Fluid Mech. 42 (1992) 189–211; J.C. Miller, J.M. Rallison, Interfacial instability between sheared elastic liquids in a channel, submitted for publication]; however, we find that the structure of the perturbation flow differs from the Couette case.

A new regime with different stability properties was first observed in a companion paper [J.C. Miller, J.M. Rallison, Interfacial instability between sheared elastic liquids in a channel, submitted for publication]. In this *narrow-core* regime the fraction of the channel occupied by the inner fluid is small and the wavenumber is large. We examine the corresponding distinguished limit and demonstrate that instability can occur at intermediate wavenumbers in flow geometries for which the long-wave and short-wave limits are both stable, contradicting some literature claims [P. Laure, H.L. Meur, Y. Demay, J.C. Saut, S. Scotto, Linear stability of multilayer plane Poiseuille flows of Oldroyd-B fluids, J. Non-Newtonian Fluid Mech. 71 (1997) 1–23; S. Scotto, P. Laure, Linear stability of three-layer Poiseuille flow for Oldroyd-B fluids, J. Non-Newtonian Fluid Mech. 83 (1999) 71–92]. The wavespeed of this mode can be substantially higher than the speed of the base flow. The perturbation grows on the time-scale of the shorter relaxation time of the two fluids. Although most of the analysis is performed for asymptotically large Weissenberg numbers, the instability is found to persist for values which should be experimentally accessible. For core-annular pipe flow the curvature of the unperturbed interface plays a role, and the stability characteristics of channel and pipe flow are found to be qualitatively different. In addition, we find some new instabilities in channel flow which fall outside the categories previously identified. We demonstrate finally that on symmetry grounds analogous narrow-core instabilities must arise for a wider class of elastic constitutive properties than Oldroyd-B.

Keywords: Elastic instability; Interfacial instability; Channel flow; Pipe flow; Coextrusion

1. Introduction

We consider the stability of symmetric three-layer Poiseuille flow, a *coextrusion flow*, of two inertialess elastic fluids in a channel as sketched in Fig. 1. The fluids are of Oldroyd-B or UCM type with matched viscosities but different relaxation time τ. The channel has width $2L$ and the velocity at the center is U_0. The inner fluid with relaxation time τ_1 occupies a fraction Δ of the channel width. We also study the analogous axisymmetric core-annular flow in a pipe.

Flows in elastic fluids may be classified on the basis of the Weissenberg number $Wi = U_0\tau_1/L$. In our context, Wi is best thought of as the ratio of the relaxation length scale $U_0\tau_1$ to the channel width L. We are concerned here with flows for which $Wi \gg 1$.

Previous work for a pipe [2,6,7] as well as for a channel [1,8,9] has concentrated on limits in which the wavelength is long or short compared to the channel width. These investigations have implicitly made the additional assumption that the wavelength is long or short compared to the distance travelled by the fluid in a relaxation time. The short-wave modes are known to have

* Corresponding author.
E-mail address: jomiller@lanl.gov (J.C. Miller).
[1] Los Alamos Report LA-UR-06-0421.

0377-0257/$ – see front matter © 2007 Elsevier B.V. All rights reserved.
doi:10.1016/j.jnnfm.2007.01.008

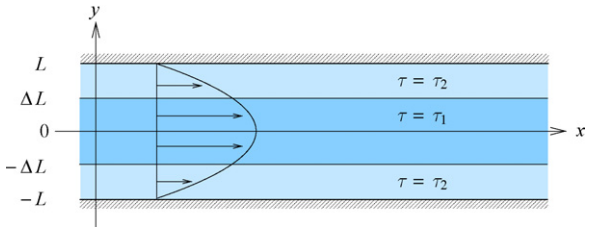

Fig. 1. Coextrusion of two elastic fluids in a channel. The two Oldroyd-B or UCM fluids differ in relaxation time τ. There is no surface tension. The base flow profile is $U = U_0(1 - y^2/L^2)$.

two distinct behaviors, depending on the size of the Weissenberg number [1–3].

Several sample computations led to the claim in [4] that, for the geometry of Fig. 1, if the long- and short-wave limits are both stable then there is stability for all wavenumbers. This claim was repeated in [5] for three non-symmetric layers. The fundamental assertion behind this claim is that all the instabilities of this geometry can be understood in the context of either long- or short-waves. We find that in general this is false.

Recent work in a companion paper [3] concerning purely elastic interfacial instabilities in Couette flow has shown that there are three significant length scales for elastic fluids with relaxation: the channel width L, the wavelength k^{-1}, and the relative distance that fluid particles travel in a relaxation time $U_0\tau_1$. It was found that rather than classifying Couette modes into long- and short-wave modes, it is more appropriate to classify them by the longest of these three length scales. The classifications are thus *long-wave* for which the wavelength is the longest, *wide-channel*, for which the channel width is the longest, and *fast-flow* for which the distance travelled in a relaxation time is the longest. In this context the two short-wave behaviors observed by previous authors are distinct; short-wave modes at large Wi are a subset of the fast-flow modes, while short-wave modes at small Wi are a subset of the wide-channel modes. It was also shown in [3] that there is an additional class of modes present in Poiseuille flow when the relaxation length is the longest length scale and the interface is close to the centerline. We refer to these as *narrow-core* modes and they are the principal subject of this paper. Further, we find some additional instabilities which do not fit into any of these classifications; these are discussed at the end of the paper.

We first review previous results for our geometry. In both channels and pipes, the long-wave criteria are derived by noting that, because the wavelength is long compared to the length over which the elastic stress relaxes, the fluids behave as if Newtonian except for a difference in elastic stress at the interface. Consequently, the results apply more generally than to just UCM or Oldroyd-B fluids. The criterion for stability of long-waves in a channel was found by Wilson [8]. Varicose long-wave modes are unstable if $(\Delta - \sqrt{2} + 1)(\tau_2 - \tau_1) > 0$, that is, if the fraction Δ occupied by the inner fluid is less than $\sqrt{2} - 1$ and it is more elastic, or the fraction occupied by the inner fluid is greater than $\sqrt{2} - 1$ and it is less elastic. For all Δ, sinuous long-wave modes are unstable if the outer fluid is more elastic and stable otherwise. A similar criterion was found by Hinch et al. [7] for axisymmetric core-annular pipe flow.

In Couette flow, the wide-channel stability is determined by effects close to the interface. In Poiseuille flow, so long as the interface is not close to the walls or the centerline, local effects do not distinguish between Couette and Poiseuille flows, and so they have the same behavior. Wide-channel stability has previously been studied in the special case of low Wi short-waves. The stability criterion for UCM fluids was found by Renardy [1] for Couette flow and the same criterion was found for core-annular Poiseuille pipe flow by Chen and Joseph [2]. Wilson and Rallison [9] found the Couette stability criterion for Oldroyd-B fluids. All of these studies considered the case $L \gg U_0\tau_1 \gg k^{-1}$, although the analysis applies to $L \gg k^{-1} \gg U_0\tau_1$ with the same result. These flows are unstable if the fluids differ, but their growth rates approach zero as Wi decreases.

Fast-flow modes have been studied previously in the special case of large Wi short-waves with $U_0\tau_1 \gg L \gg k^{-1}$. These have the same stability as Couette modes, again so long as the interface is sufficiently far from the walls or centerline. The corresponding UCM results were found for Couette flow by Renardy [1] and the same results were found for core-annular pipe Poiseuille flow by Chen and Joseph [2]. There is instability when the two relaxation times differ but are not too different (i.e., $\tau_2 \neq \tau_1$ and $\xi_c^{-1} > \tau_2/\tau_1 > \xi_c$ where $\xi_c \approx 0.28$). Wilson and Rallison [9] showed that Oldroyd-B fluids with sufficient Newtonian viscosity give instability whenever the relaxation times differ. It was shown in [3] that the Couette stability properties of UCM and Oldroyd-B fluids do not change if $U_0\tau_1 \gg k^{-1} \gg L$, that is, if the wavelength is long compared to the channel width but still short compared to the relaxation length scale. In this paper we find that Poiseuille modes in this limit also have the same stability properties, though the mode structure is qualitatively different from that of Couette modes. Consequently we refer to these modes as *Couette-like fast-flow modes*.

A new class of fast-flow modes appears in Poiseuille flow. The Couette-like fast-flow growth rate is governed by a boundary layer at the interface with thickness $1/kU'\tau$. If U'/U'', the length over which the shear rate changes by an amount comparable to itself, is of the same order as the boundary layer thickness then the boundary layer structure is affected and the stability properties change. At the interface the ratio of these two length scales for Poiseuille flow is proportional to $kU_0\tau\Delta^2$. When this ratio is large (i.e., the interface is sufficiently far from the centerline) the Couette-like fast-flow modes are found. However, when $\Delta \sim (U_0\tau k)^{-1/2}$, a new *narrow-core* regime emerges which has not been examined previously. In either case, the effect of the wall on the stability disappears provided that the boundary layer thickness is small compared to the distance of the interface from the wall, that is, if $kU_0\tau\Delta(1 - \Delta) \gg 1$. In the narrow-core case only the dimensionless group $\Delta(U_0\tau k)^{1/2}$ and the ratio of relaxation times enter the problem. The narrow-core instability is found to persist for some parameter values when the length scales are not well-separated (because the Weissenberg number is not large or the wavelength is comparable to the channel width). It can give rise to instabilities for values of Δ and Wi which are known to be stable to long-wave

Please cite this article in press as: J.C. Miller, J.M. Rallison, Instability of coextruded elastic liquids at high Weissenberg number, J. Non-Newtonian Fluid Mech. (2007), doi:10.1016/j.jnnfm.2007.01.008

and wide-channel modes as well as to Couette-like fast-flow modes.

This paper is organized as follows: in Section 2 we introduce the governing equations. In Section 3 we discuss the modifications of the Couette fast-flow regime found in Poiseuille flow. Section 4 contains the bulk of our results and investigates the narrow-core instabilities in channel flow. Section 5 extends these results in a core-annular pipe geometry. Section 6 discusses other instabilities we have found which fall outside our classification. Finally in Section 7 we discuss implications of our results.

2. Governing equations

We first consider two Oldroyd-B fluids in pressure-driven flow through a two-dimensional channel as shown in Fig. 1. The walls are at $y = \pm L$ and the interfaces at $y = \pm \Delta L$. The inertialess equations governing the flow are

$$\nabla \cdot \Sigma = 0 \tag{1}$$

$$\Sigma = -P\mathsf{I} + \mu\left(2\beta\mathsf{E} + \frac{1-\beta}{\tau}\mathsf{A}\right), \tag{2}$$

$$(\partial_t + \boldsymbol{U}\cdot\nabla)\mathsf{A} - [\nabla\boldsymbol{U}]^{\mathrm{T}}\cdot\mathsf{A} - \mathsf{A}\cdot[\nabla\boldsymbol{U}] = \frac{1}{\tau}(\mathsf{I}-\mathsf{A}), \tag{3}$$

$$\mathsf{E} = \frac{(\nabla\boldsymbol{U}) + (\nabla\boldsymbol{U})^{\mathrm{T}}}{2}, \tag{4}$$

$$\nabla\cdot\boldsymbol{U} = 0 \tag{5}$$

where Σ is the stress which depends on the elastic strain A and the rate of strain E . $\boldsymbol{U}$ is the fluid velocity. The fluids have matched constant shear viscosity μ, divided into elastic and Newtonian contributions by the parameter β. The fluids differ because they have different relaxation times τ_1 and τ_2. When $\beta = 0$ the fluids are Upper Convected Maxwell (UCM), while $\beta = 1$ gives two identical Newtonian fluids.

We apply no-slip conditions

$$\boldsymbol{U} = 0$$

at the walls. At the interfaces, the velocity must be continuous and so

$$[\![\boldsymbol{U}]\!] = 0,$$

where $[\![\cdot]\!]$ denotes the change in the bracketed quantity across the interface. Additionally, in the absence of surface tension we have

$$[\![\Sigma]\!]\cdot\boldsymbol{N} = 0$$

where $\boldsymbol{N}$ is the unit normal pointing into the outer fluid.

For axisymmetric core-annular pipe flow with walls at $r = L$ and interface at $r = \Delta L$ the equations are unchanged and a regularity condition is applied at $r = 0$.

2.1. The unperturbed flow

For the unperturbed flow, $(\partial_t + \boldsymbol{U}\cdot\nabla)\mathsf{A} = \mathsf{0}$. The elastic stress is given by

$$\mathsf{A} = \begin{pmatrix} 1+2\tau^2U'^2 & \tau U' \\ \tau U' & 1 \end{pmatrix},$$

with $U(y) = U_0(1 - y^2/L^2)$ for channel flow.

For pipe flow in (r, θ, z) coordinates we similarly find

$$\mathsf{A} = \begin{pmatrix} 1 & 0 & \tau U' \\ 0 & 1 & 0 \\ \tau U' & 0 & 1+2\tau^2U'^2 \end{pmatrix},$$

and $U(r) = U_0(1 - r^2/L^2)$.

In Appendix A we derive the linear perturbation equations for modes proportional to $\exp(\mathrm{i}kx - \mathrm{i}\omega t)$ for real k and complex ω. We use lowercase letters to denote perturbations to their uppercase counterparts.

2.2. Non-dimensionalization in the limit $Wi \gg 1$

As in [3], the scalings appropriate for large Wi flows are non-standard. We derive the non-dimensionalized channel equations, using asterisks to denote dimensionless quantities. The pipe equations are non-dimensionalized similarly.

In Section 1 we noted that if $\Delta \sim (U_0\tau k)^{-1/2}$ we encounter the narrow-core regime. This motivates our choice of cross-stream length as

$$y^* = \frac{(U_0\tau_1 k)^{1/2}}{L}y.$$

We rescale times by τ_1 so that $\tau_1^* = 1$. The outer fluid then has relaxation time $\tau_2^* = \xi = \tau_2/\tau_1$. The complex frequency ω becomes $\omega^* = \tau_1\omega$.

We non-dimensionalize k^{-1} and x with the length scale $U_0\tau_1$, representing the distance the fluid travels during a relaxation time. Thus,

$$k^* = U_0\tau_1 k,$$
$$x^* = \frac{x}{U_0\tau_1}.$$

It is convenient to use a streamfunction ψ so that $\boldsymbol{u} = (\mathrm{D}\psi, -\mathrm{i}k\psi)$ where 'D' denotes differentiation with respect to y. We rescale ψ so that

$$\psi^* = \psi k^2\tau_1 = k^{*2}\frac{\psi}{U_0^2\tau_1}.$$

The interface perturbation δ is non-dimensionalized with respect to k

$$\delta^* = k\delta.$$

The a_{ij} measuring elastic strain perturbation are already dimensionless, but we rescale them as

$$a_{11}^* = a_{11}\left(\frac{kL}{Wi}\right)^{3/2}, \tag{6}$$

Please cite this article in press as: J.C. Miller, J.M. Rallison, Instability of coextruded elastic liquids at high Weissenberg number, J. Non-Newtonian Fluid Mech. (2007), doi:10.1016/j.jnnfm.2007.01.008

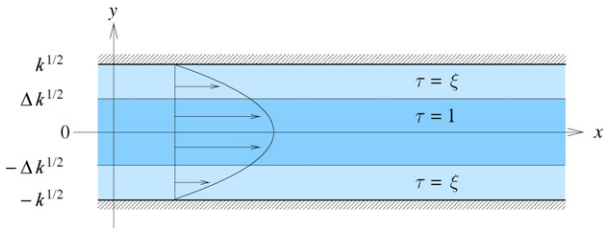

Fig. 2. The non-dimensionalized base flow.

$$a_{12}^* = a_{12}\left(\frac{kL}{Wi}\right), \tag{7}$$

$$a_{22}^* = a_{22}\left(\frac{kL}{Wi}\right)^{1/2}. \tag{8}$$

We now drop asterisks. The rescaled baseflow is shown in Fig. 2. We write the leading order equations in the limit that Wi is large. The neglected error terms are $\mathcal{O}(kWi^{-2})$.

The vorticity equation (A.1) becomes

$$\frac{\beta\tau}{1-\beta}\mathrm{D}^4\psi + \mathrm{D}^2 a_{12} + \mathrm{i}\mathrm{D}a_{11} = 0, \tag{9}$$

while the constitutive equations (A.2) become

$$\alpha a_{11} = -4ya_{12} + 16\mathrm{i}\tau^2 y^2 \mathrm{D}\psi - 4\tau y\mathrm{D}^2\psi + 16\mathrm{i}\tau^2 y\psi, \tag{10}$$

$$\alpha a_{12} = -2ya_{22} + \mathrm{D}^2\psi + 8\tau^2 y^2\psi - 2\mathrm{i}\tau\psi, \tag{11}$$

$$\alpha a_{22} = -4\tau y\psi - 2\mathrm{i}\mathrm{D}\psi \tag{12}$$

where

$$\alpha = -\mathrm{i}\omega + \mathrm{i}k - \mathrm{i}y^2 + \frac{1}{\tau}. \tag{13}$$

At the interface $y = \Delta k^{1/2}$ the velocity continuity (A.7) and (A.8) and force balance (A.9) and (A.10) become

$$[\![\psi]\!]_{\Delta k^{1/2}} = 0, \tag{14}$$

$$[\![\mathrm{D}\psi]\!]_{\Delta k^{1/2}} = 0, \tag{15}$$

$$\left[\!\!\left[\frac{\beta}{1-\beta}\mathrm{D}^2\psi - 8\mathrm{i}y^2\tau\delta + \frac{a_{12}}{\tau}\right]\!\!\right]_{\Delta k^{1/2}} = 0, \tag{16}$$

$$\left[\!\!\left[\frac{\beta}{1-\beta}\mathrm{i}\mathrm{D}^3\psi + \frac{\mathrm{i}\mathrm{D}a_{12}}{\tau} - \frac{a_{11}}{\tau}\right]\!\!\right]_{\Delta k^{1/2}} = 0, \tag{17}$$

and the kinematic boundary condition (A.6) becomes

$$(-\mathrm{i}\omega + \mathrm{i}k - \mathrm{i}y^2)\delta = -\mathrm{i}\psi. \tag{18}$$

The boundary conditions (A.3) at the wall $y = k^{1/2}$ are

$$\psi = \mathrm{D}\psi = 0 \tag{19}$$

while the conditions (A.4) and (A.5) at the center $y = 0$ become

$$\mathrm{D}\psi = \mathrm{D}^3\psi = 0 \qquad \text{(sinuous)}, \tag{20}$$

$$\psi = \mathrm{D}^2\psi = 0 \qquad \text{(varicose)}. \tag{21}$$

Setting $\Omega = \omega - k$ eliminates the wavenumber k except in determining the location of the interface and the walls. At large k the walls are far from the interface and have no effect on the growth rate. If $\Delta k^{1/2}$ is also large so that the interface is not close to the center (and the shear rate is effectively constant) we expect the same stability characteristics as for Couette flow determined in [3]. However, if $\Delta k^{1/2}$ is not large, narrow-core modes appear.

2.3. Numerical methods

We are unable to solve the eigenvalue problem defined by Eqs. (9)–(21) analytically, and so we use a shooting algorithm and a Chebyshev spectral algorithm both described in [3]. The two algorithms reproduce results from [8–11]. In general they give consistent results, but the shooting algorithm sometimes fails to converge if either k becomes large or both Δ and k become small. If $\Delta k^{1/2}$ is large, the spectral method requires high resolution. These difficulties lead to lacunae in the figures presented for some parameter values.

3. Couette-like fast-flow instabilities in channel coextrusion flow (Δ fixed and $Wi, k \gg 1$)

For fast-flow the relaxation length is long compared to both the wavelength and the channel width. There are two subclasses. When the wavelength is shorter than the channel width the perturbation flow decays exponentially within a wavelength of the interface. The results of Renardy [1] and Chen and Joseph [2] for Couette flow apply immediately in this case. However, when the wavelength is longer than the channel width, the perturbation flow is not localized at the interface. The stability criteria found in Couette flow [3] persist in Poiseuille flow as long as $\Delta k^{1/2} \gg 1$, but the mode structure is modified as described below.

3.1. UCM fluids

Fig. 3 shows the perturbation flow for sinuous and varicose modes with $\xi = 0.5$, $\Delta = 0.7$, and $k = 30$. In both cases, the flow decays exponentially in the less elastic outer fluid, but is everywhere of order unity in the inner fluid. This mode structure differs from that of Couette flow for which the perturbation flow is of order unity throughout both fluids. On the other hand, the value of ω predicted by the Couette calculation [3] is $\omega = (1-\Delta^2)k + 0.30544 + 0.06603\mathrm{i} + \mathcal{O}(1/k) = 15.60544 + 0.06603\mathrm{i} + \mathcal{O}(1/k)$, and our calculated results are in close agreement: for the varicose mode $\omega = 15.6203 + 0.0598\mathrm{i}$, while $\omega = 15.6208 + 0.0590\mathrm{i}$ for the sinuous mode. Thus, as far as the growth rates are concerned, the two interfaces do not interact despite the fact that the perturbation flow does not decay between them: the Couette calculation for a single interface suffices.

The velocity plots in Fig. 3 suggest the existence of a boundary layer close to the center. The flux in this boundary layer plays a role in preventing the interfaces from interacting. We can see this more clearly by choosing a different geometry that eliminates the lower interface, giving an asymmetric base flow for which a single fluid occupies $-k^{1/2} < y < \Delta k^{1/2}$. The resulting perturbation flow is shown in Fig. 4 for $\xi = 0.5$,

Please cite this article in press as: J.C. Miller, J.M. Rallison, Instability of coextruded elastic liquids at high Weissenberg number, J. Non-Newtonian Fluid Mech. (2007), doi:10.1016/j.jnnfm.2007.01.008

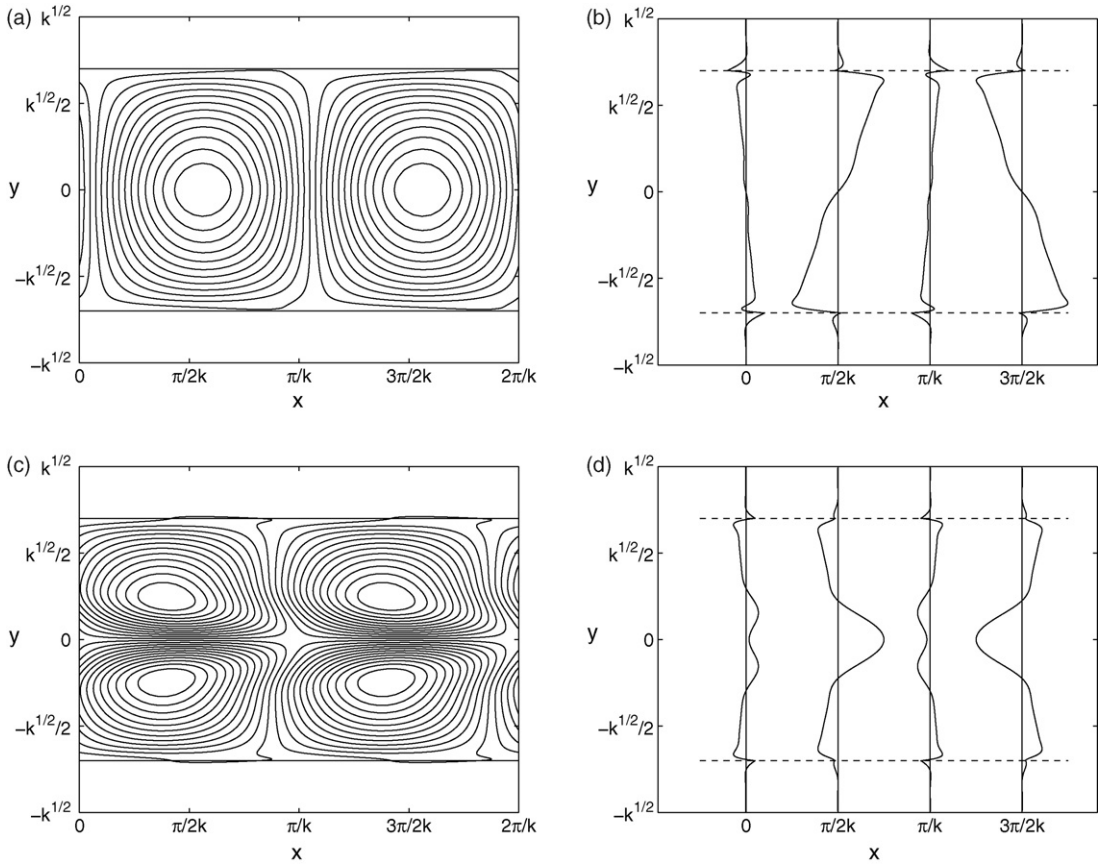

Fig. 3. UCM fluids. Perturbation flows for sinuous and varicose channel modes for $\xi = 0.5$, $\Delta = 0.7$, and $k = 30$. Walls are at $y = \pm k^{1/2}$, and interfaces at $y = \pm\Delta k^{1/2}$. (a) Streamlines for sinuous mode. (b) Perturbed sinuous x-velocity. (c) Streamlines for varicose mode. (d) Perturbed varicose x-velocity.

$\Delta = 0.7$ with $k = 30$ and $k = 500$. For $k = 30$, the value of ω is $\omega = 15.6205 + 0.0594\mathrm{i}$, close to the prediction above, while for $k = 500$, it is $\omega = 255.3063 + 0.0657\mathrm{i}$, which matches the predicted value of $\omega = 255.30544 + 0.06603\mathrm{i} + \mathcal{O}(1/k)$ well. The boundary layer close to the center allows for a return flow which keeps the net flux zero without requiring a flow in the upper fluid or the lower half-channel.

A more rigorous argument showing that the large k limit of Poiseuille fast-flow modes have the same growth rates as for Couette fast-flow modes is found in [12].

3.2. Oldroyd-B fluids

Fast-flow Oldroyd-B modes were studied in [9] with the wavelength short compared to the channel width. As β increases, the range of ξ giving instability increases. For sufficiently large $\beta < 1$ instability exists for all ξ. This result was also observed for $U_0\tau_1 \gg k^{-1} \gg L$ in [3]. The same behavior occurs for Poiseuille flow (demonstrated later in Fig. 18). However, as for UCM fluids, the structure of the mode changes.

4. Narrow-core instabilities in channel coextrusion flow ($Wi \gg 1$, $\Delta \sim k^{-1/2}$)

When the interfaces are sufficiently close to the center, the variation in the base shear rate across the boundary layer affects the stability properties and can lead to instabilities distinct from those of Couette flow [3]. These new instabilities can occur at intermediate wavenumbers, even when both small and large wavenumber modes are stable.

For example, Fig. 5(a) shows the growth rates of varicose modes for $\xi = 0.2$ and $\Delta = 0.5$, parameters for which both sinuous and varicose modes are stable as $k \to 0$ and $k \to \infty$. Fig. 5(b) shows the growth rates of sinuous modes for $\xi = 0.2$ and $\Delta = 0.3$, for which sinuous modes are stable as $k \to 0$ and $k \to \infty$. Both cases have instability at intermediate k. The behavior can be more complicated [Fig. 5(c and d)], with multiple unstable modes or multiple regions of instability for a single mode. These instabilities frequently (but not always) travel faster than the centerline of the base flow, so effects beyond advection of material would be needed to understand the instability mechanism.

We plot contours of the maximum growth rate in (k, Δ) space for different ξ in Fig. 6 showing the long-wave varicose instability ($k \to 0, \Delta < \sqrt{2} - 1$) and Couette-like fast-flow instabilities (Δ fixed, $k \to \infty, \xi > \xi_c$). There is also evidence of a $\Delta \sim k^{-1/2}$ scaling, corresponding to the new narrow-core regime which can be unstable for both sinuous and varicose modes.

We now investigate the narrow-core instabilities in more detail for both UCM and Oldroyd-B fluids. We later confirm numerically that these instabilities appear in the distinguished limit $k \to \infty$, $\Delta k^{1/2} \sim 1$ for which the effect of the walls is

Please cite this article in press as: J.C. Miller, J.M. Rallison, Instability of coextruded elastic liquids at high Weissenberg number, J. Non-Newtonian Fluid Mech. (2007), doi:10.1016/j.jnnfm.2007.01.008

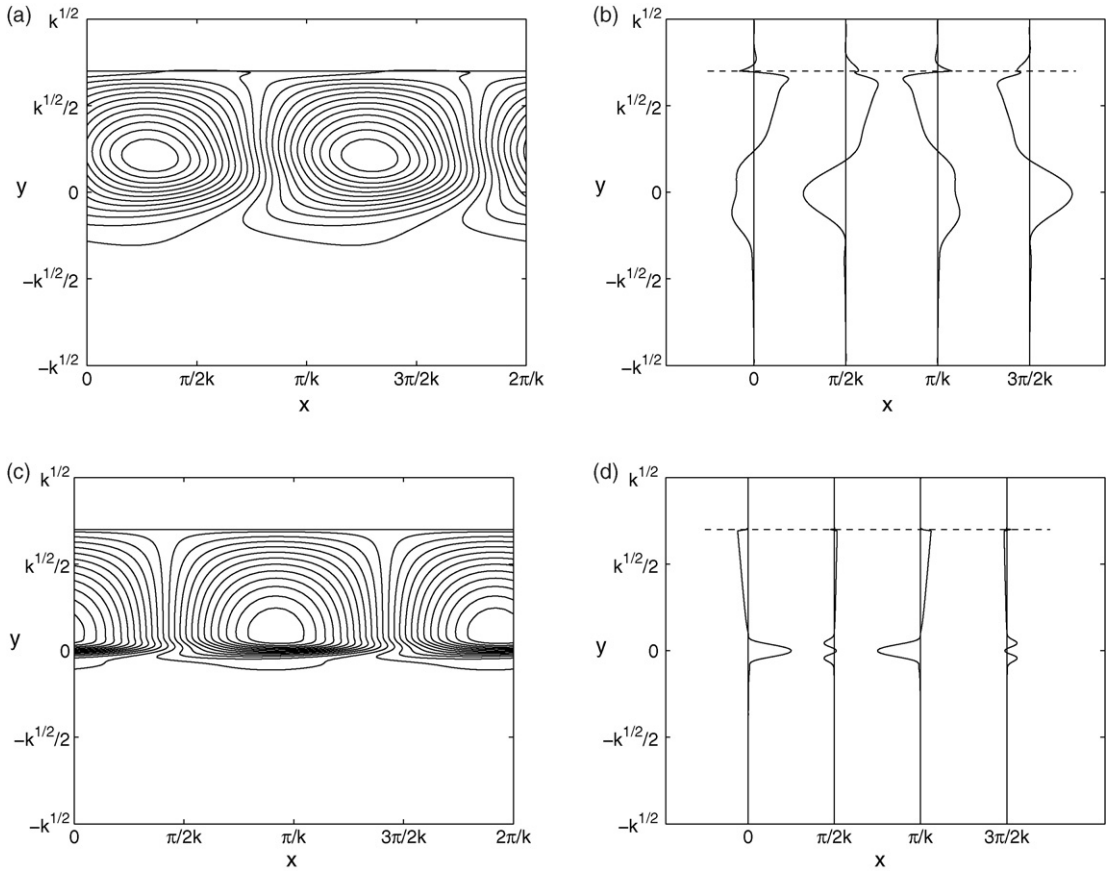

Fig. 4. Perturbation flows for UCM Poiseuille flow in a channel with a single interface at $y = \Delta k^{1/2}$ with $\xi = 0.5$, $\Delta = 0.7$, and $k = 30$ or 500. (a) Streamlines: $k = 30$. (b) Perturbed x-velocity: $k = 30$. (c) Streamlines: $k = 500$. (d) Perturbed x-velocity: $k = 500$.

negligible. If k is decreased (and Δ increased keeping $\Delta k^{1/2}$ fixed), the effect of the walls grows, but instability can persist for k as small as 5.

4.1. UCM fluids

4.1.1. Instability at moderate k

We first consider varicose modes. The plots of Fig. 6 show that the growth rates of modes in (k, Δ) space for fixed ξ have an unstable *tongue* in the marginal stability curve at $k \approx 5$. In Fig. 7 similar plots for smaller ξ show multiple unstable tongues. Our results suggest that the maximum number of tongues for UCM fluids is three. As ξ increases, the tongues progressively disappear until at $\xi \approx 0.56$ there are no tongues and there is stability at moderate k for $\Delta > \sqrt{2} - 1$ (the $k \to 0$ varicose stability boundary).

These tongues identify the smallest values of k for which narrow-core instabilities exist. They are of particular significance because they give values of Δ for which both $k \to 0$ and $k \to \infty$ limits are stable, but instability arises at moderate k [e.g., Fig. 6(a) for $\Delta = 0.5$].

In Fig. 7 we see that as ξ increases beyond 0.09 the second tongue merges with the first, whereas if ξ becomes small it migrates to larger values of k. The local maxima of the marginal stability curve locate the position of the tongues. We plot the values of the first two local maxima in Fig. 8(a). When $\xi = 0.069$ the first two tongues are marginally stable at $\Delta = 0.6023$, and so for these parameters there are two nonzero wavenumbers which are marginally stable, shown in Fig. 8(b). As Δ decreases below 0.6023 two varicose instabilities with different wavenumber arise. Consequently there is a codimension-2 bifurcation for this set of parameters.

We turn now to sinuous modes. For moderate k, Fig. 6 shows that if ξ is sufficiently large, the flow is stable to narrow-core modes. However, when ξ is small, more than one unstable mode exists, seen in Fig. 5(d) and in Fig. 9 both for $\xi = 0.025$. Both unstable modes have the $\Delta \sim k^{-1/2}$ scaling. The two modes have substantially different growth rates. The faster growing mode has a wavespeed greater than the base flow velocity at the centerline of the channel.

4.1.2. Instability at large k

When k is large and Δ is small, the influence of the walls at $y = k^{1/2}$ becomes unimportant. The complex frequency ω scales like $k + \mathcal{O}(1)$, and so neither α [Eq. (13)] nor the kinematic boundary condition [Eq. (18)] depend on k. The only appearance of k or Δ in the problem is in the combination $\Delta k^{1/2}$. Consequently we anticipate that the complex growth rate depends only on ξ and $\Delta k^{1/2}$. Fig. 10 verifies this by showing that for the fastest growing mode $\Delta k^{1/2}$ is fixed as $k \to \infty$. This implies

Please cite this article in press as: J.C. Miller, J.M. Rallison, Instability of coextruded elastic liquids at high Weissenberg number, J. Non-Newtonian Fluid Mech. (2007), doi:10.1016/j.jnnfm.2007.01.008

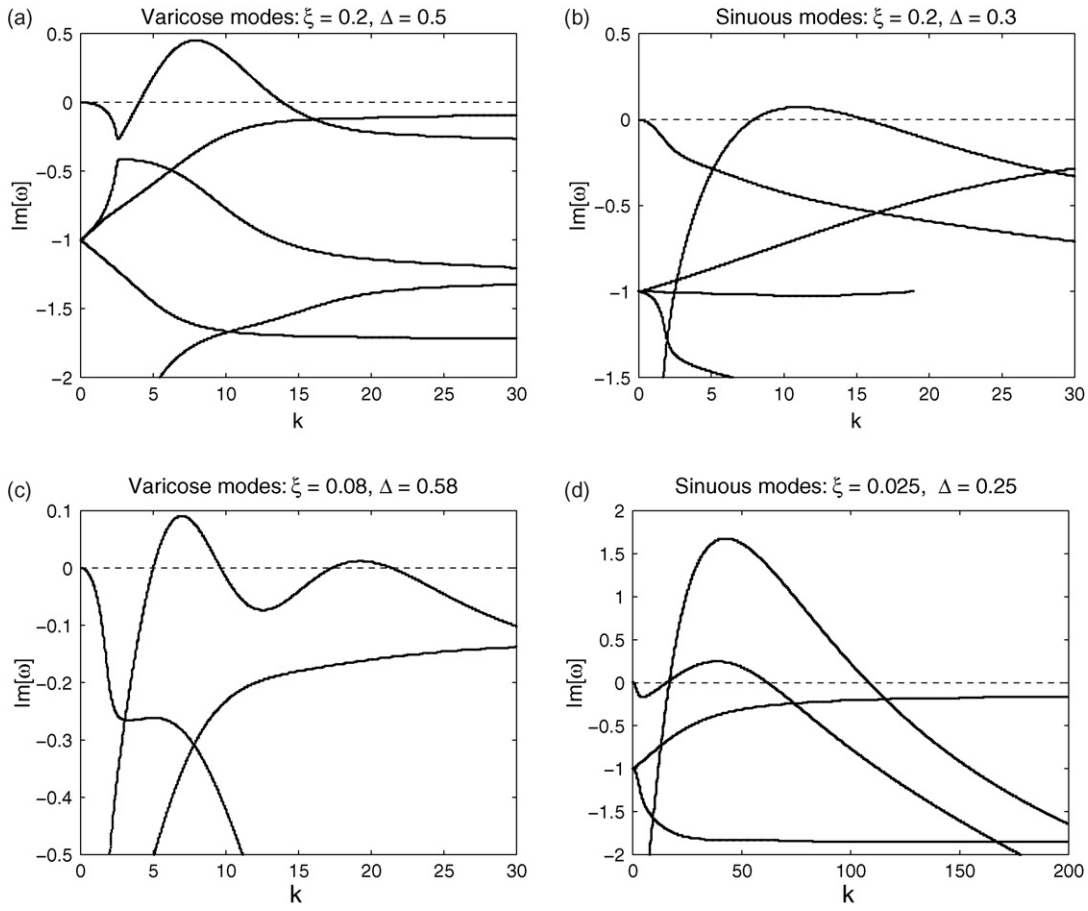

Fig. 5. Sample dispersion relations for UCM channel flows. (a) Growth rates of varicose modes for $\xi = 0.2$, $\Delta = 0.5$ with $Wi \gg 1$ showing instability only for intermediate wavenumbers. (b) Growth rates of sinuous modes for $\xi = 0.2$, $\Delta = 0.3$ with $Wi \gg 1$. Note that a mode enters the continuous spectrum at $k \approx 20$ (see [11]). (c) Growth rates of varicose modes for $\xi = 0.08$, $\Delta = 0.58$. Two distinct ranges of k are unstable for the same mode. (d) Growth rates of sinuous modes for $\xi = 0.025$, $\Delta = 0.25$. Two distinct modes are unstable.

that in an experiment with small Δ the fastest growing mode has $k \propto \Delta^{-2}$.

Fig. 11 shows for this distinguished limit the marginal stability curves at large k for the full range $0 < \xi < \infty$, with a rescaling of the axis for $\xi > 1$. As $\xi \to 0$ the narrow-core instability exists for any value of $\Delta k^{1/2}$. If $\Delta k^{1/2} \approx 1$, the growth rates are found to become large. There is a small island of stability for $\xi \approx 0.06$, $\Delta k^{1/2} \approx 2$. In an experimental flow for which Δ is fixed but k can vary, this island will manifest itself as a window of wavelengths for which varicose modes are stable surrounded by unstable wavelengths.

As ξ is increased past $\xi_c \approx 0.28$ a further varicose instability appears for sufficiently large $\Delta k^{1/2}$. This is the Couette-like fast-flow instability discussed previously in Section 3. For ξ below, but sufficiently close to, 1 the fast-flow mode is stable.

The growth rate must be zero at $\xi = 1$ (because the fluids are identical) and generically crosses zero as ξ passes through 1. In Fig. 11 stability reverses moving from $\xi \to 1^-$ to $\xi \to 1^+$. That is, if the flow is stable [unstable] with a slightly more elastic inner fluid, then making the outer fluid slightly more elastic destabilizes [stabilizes] the flow. When $1 < \xi < \xi_c^{-1} \approx 3.6$ the Couette-like fast-flow instability is present at sufficiently large $\Delta k^{1/2}$ and is not clearly distinguished from the narrow-core instability. As ξ increases past ξ_c^{-1}, the unstable region shrinks rapidly, but does not disappear as $\xi \to \infty$. For sufficiently small $\Delta k^{1/2}$ there is stability for any $\xi > 1$.

We show in the same manner the stability to sinuous perturbations in Fig. 12. As in the varicose case, we find the Couette-like fast-flow instability at sufficiently large $\Delta k^{1/2}$ if $\xi_c < \xi < \xi_c^{-1}$ unless $\xi = 1$, but there is a narrow-core instability for small ξ. This sinuous narrow-core instability is qualitatively different from the varicose narrow-core instability in that it has much larger growth rates and a maximum value of ξ of about 0.25. When ξ is greater than 1, a similar picture emerges to the varicose modes, except that there is no stable region at small $\Delta k^{1/2}$. There is no analogue of the island of stability found in varicose modes. The sinuous marginal stability curve passes through the stable varicose island, and so part of the island corresponds to a region of instability to sinuous modes but stability to varicose modes while part of it is stable to both.

At small values of ξ the varicose growth rate diverges like $\ln(\xi)$, while the sinuous growth rates diverge like $1/\xi$, with a correction which appears to be logarithmic in ξ. In consequence, when the relaxation time of the outer fluid is short compared to the inner relaxation time, instabilities grow on the short timescale of the outer fluid. If we rescale time so that the outer

Please cite this article in press as: J.C. Miller, J.M. Rallison, Instability of coextruded elastic liquids at high Weissenberg number, J. Non-Newtonian Fluid Mech. (2007), doi:10.1016/j.jnnfm.2007.01.008

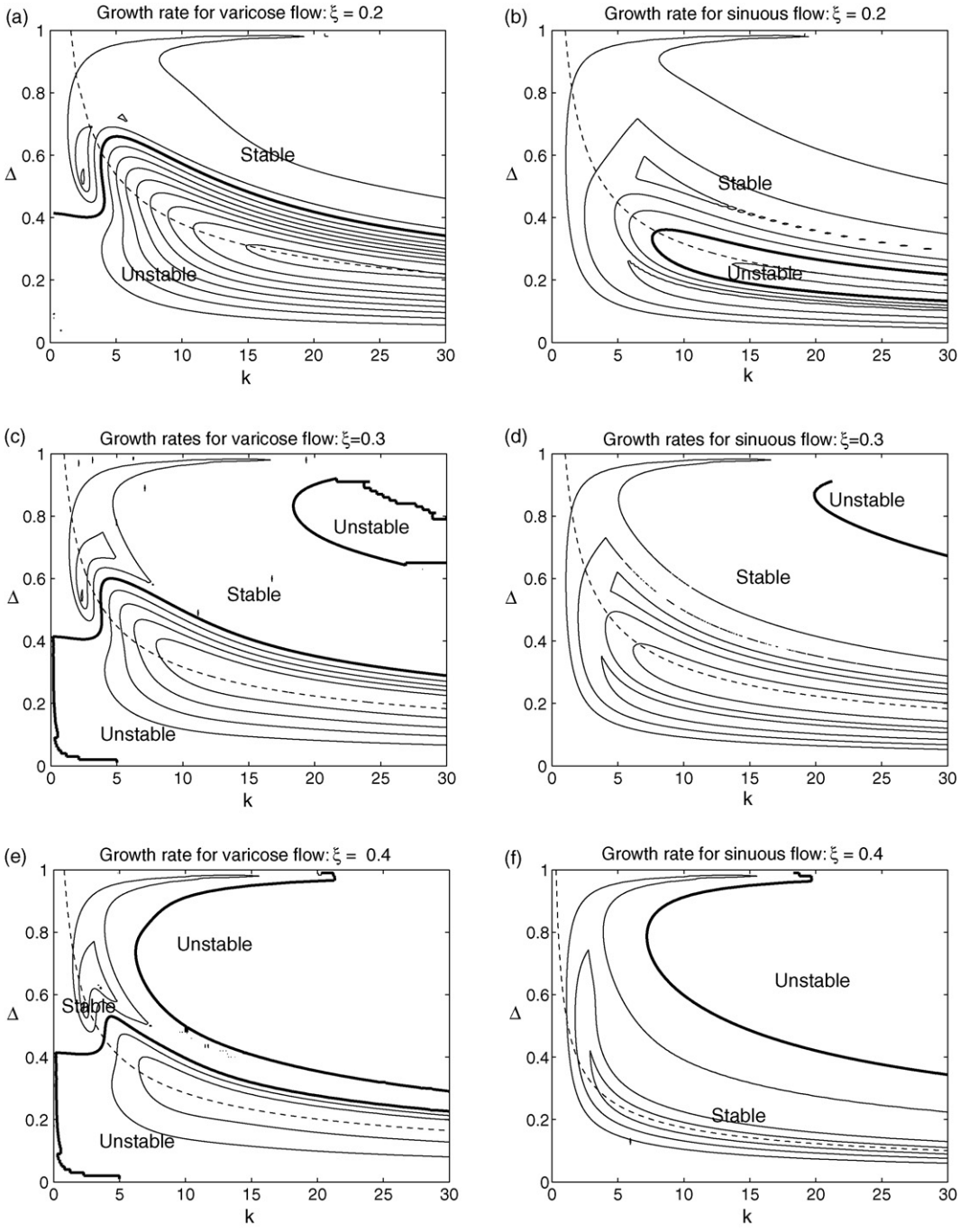

Fig. 6. Equally spaced contours of UCM channel mode growth rates for $Wi \gg 1$. Bold contours show stability boundaries. For fixed Δ as $k \to \infty$, modes are stable [unstable] if $\xi < \xi_c \approx 0.28$ [$1 > \xi > \xi_c$]. For fixed $\Delta k^{1/2}$ (dashed lines) the narrow-core regime is found as $k \to \infty$. Numerical problems appear where parameter continuation is difficult in the lower left and upper right corners. (a) Varicose: $\xi = 0.2 < \xi_c$. (b) Sinuous: $\xi = 0.2 < \xi_c$. (c) Varicose: $\xi = 0.3 > \xi_c$. (d) Sinuous: $\xi = 0.3 > \xi_c$. (e) Varicose: $\xi = 0.4 > \xi_c$. (f) Sinuous: $\xi = 0.4 > \xi_c$.

relaxation time becomes 1 then the sinuous growth rates tend to positive constants (approximately 0.35 and 0.017) as the rescaled inner relaxation time becomes infinite. In contrast, the growth rate of the varicose mode tends to zero, as shown in Fig. 13.

4.1.3. Perturbation flow

The perturbation flow of varicose modes is of comparable magnitude throughout the channel. There is a central boundary layer with thickness $\mathcal{O}(1)$ and wall boundary layers with thickness $\mathcal{O}(k^{-1/2})$ (Fig. 14). In contrast sinuous modes may be shown to be exponentially small outside the central boundary layer (Fig. 15), see [12]. The physical reason for this is as follows: the varicose modes have a net mass flux in the central boundary layer, and so the outer region must have an opposite flux in order to satisfy conservation of mass. The only length scale available to the outer region is the width of the channel (as the wavelength is long compared to the width), and so the flow fills the channel. In contrast, the sinuous modes have no net

Please cite this article in press as: J.C. Miller, J.M. Rallison, Instability of coextruded elastic liquids at high Weissenberg number, J. Non-Newtonian Fluid Mech. (2007), doi:10.1016/j.jnnfm.2007.01.008

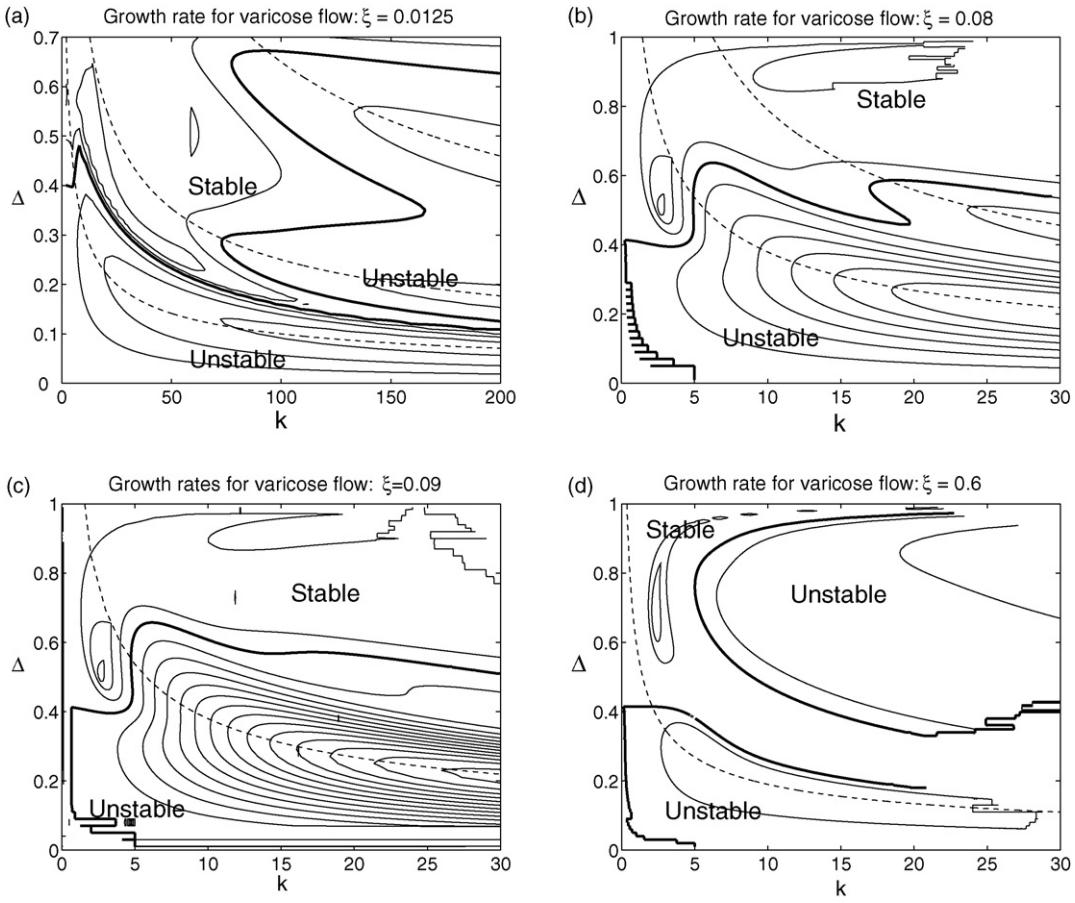

Fig. 7. Varicose mode growth rates for UCM flow in a channel. More than one unstable tongue exists at small ξ, but disappear for larger ξ. The tongues are associated with the narrow-core modes occurring at fixed $\Delta k^{1/2}$ as $k \to \infty$ (dashed lines). The shooting method has difficulties for k and Δ both small and for large k. The plot in (a) was created using the spectral method and has extended horizontal and reduced vertical axes. (a) $\xi = 0.0125$. Three tongues are present. (b) $\xi = 0.08$. Only two tongues are found. (c) $\xi = 0.09$. The second tongue has almost merged with the primary tongue. (d) $\xi = 0.6$. The tongues no longer exist.

mass flux in the central boundary layer. Thus, there is no need for flow in the outer region.

4.1.4. Wavespeed

From Eq. (13) we have $\alpha = -\mathrm{i}\omega + \mathrm{i}k - \mathrm{i}y^2 + 1/\tau$ which is $\mathcal{O}(1)$ in the central boundary layer, and so as $k \to \infty$ we must have $\omega = k + \mathcal{O}(1)$. Hence, the mode travels with velocity 1 (equal to the base flow at the center) plus an $\mathcal{O}(1/k)$ correction. Remarkably this correction can be positive, so that the wave travels faster than any point in the base flow. This is shown in Fig. 16. We conclude that advection cannot account for the mechanism.

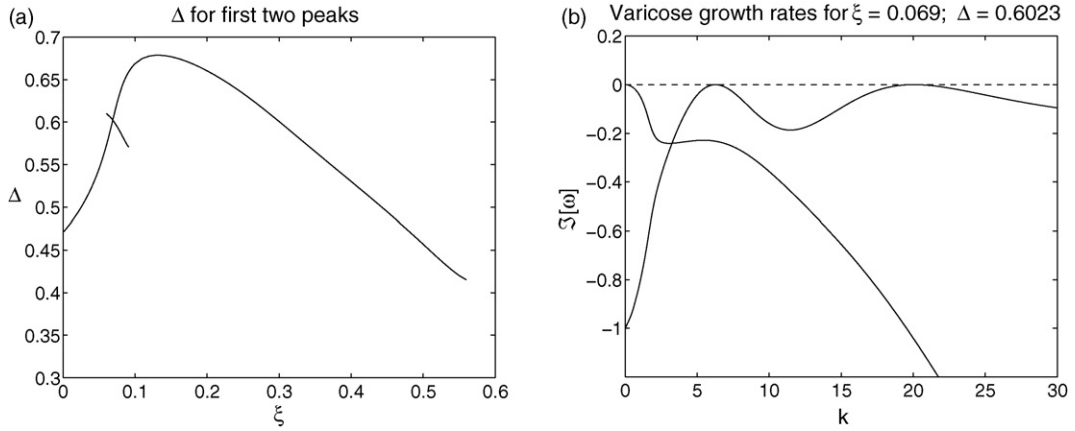

Fig. 8. Varicose modes for UCM fluids in a channel. The maxima of the tongues gives the value of Δ at which a bifurcation occurs. The second tongue only has a local maximum for a short range of ξ. At $\xi = 0.069$, $\Delta = 0.6023$ both tongues are marginally stable. (a) Value of Δ at maxima of first two tongues. (b) At $\xi = 0.069$, two bifurcations occur as Δ crosses 0.6023.

Please cite this article in press as: J.C. Miller, J.M. Rallison, Instability of coextruded elastic liquids at high Weissenberg number, J. Non-Newtonian Fluid Mech. (2007), doi:10.1016/j.jnnfm.2007.01.008

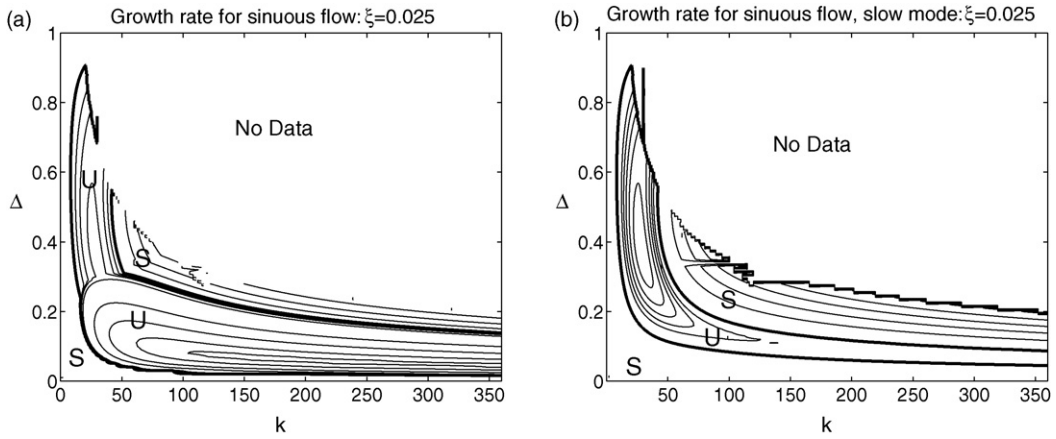

Fig. 9. When $\xi = 0.025$ there are two unstable sinuous modes. One mode travels faster than the centerline. The other travels slower than the centerline (and slower than the interface). The numerics could not resolve large values of $\Delta k^{1/2}$. (a) Growth rate of the most dangerous mode. One unstable mode obscures the other for large k. (b) Growth rate of the most dangerous mode having wavespeed less than 1.

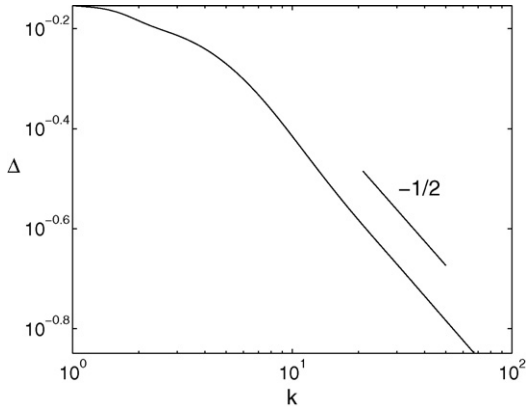

Fig. 10. UCM channel flow. Interface location for fastest growing varicose mode at each wavenumber with $\xi = 0.2$. For large k, the fastest growing mode has $\Delta \propto k^{-1/2}$.

For $\xi = 0.2$ there is a single unstable varicose mode. In Fig. 16(a) we compare its wavespeed with the corresponding interfacial velocity and the centerline velocity. The wave travels faster than the centerline. For each value of k, we have selected Δ to maximize the growth rate.

For sinuous flow we can have multiple unstable modes. We take $\xi = 0.025$ and consider two unstable modes separately. We again select Δ to maximize each growth rate, plotting the same quantities in Fig. 16(b and c) as in Fig. 16(a). In this case one mode moves substantially faster than the centerline and interface, while the other moves slower than both.

4.1.5. *Finite Wi effects*

The leading order corrections to the $Wi \gg 1$ equations of Section 2.2 are all $\mathcal{O}(kWi^{-2})$. These correction terms are often small even for moderate values of Wi; the convergence is illustrated in Fig. 17. We have found narrow-core instability for Wi as small as 4.

4.2. *Oldroyd-B fluids*

The addition of a Newtonian component of viscosity does not stabilize narrow-core modes (see Fig. 18). For comparison, we take $\xi = 0.2$. When $1 - \beta$ is not small, at least two distinct narrow-core modes are found with $\Delta \sim k^{-1/2}$. As $\beta \to 1$, the fluids become identical Newtonian fluids, and so the growth rates at fixed k must tend to zero. However, this limit is not approached

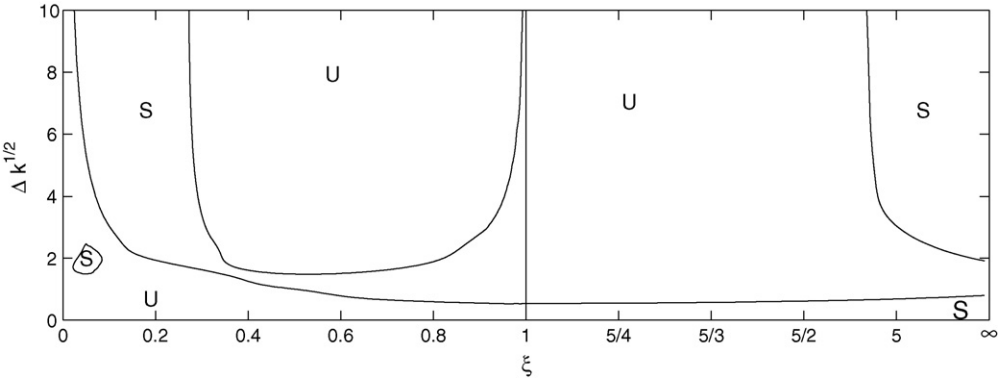

Fig. 11. Marginal stability curves for varicose narrow-core UCM channel modes. Computations are performed for $k = 4000$. U and S denote unstable and stable regions, respectively. Note that for $\xi > 1$ the ξ-axis has been rescaled.

Please cite this article in press as: J.C. Miller, J.M. Rallison, Instability of coextruded elastic liquids at high Weissenberg number, J. Non-Newtonian Fluid Mech. (2007), doi:10.1016/j.jnnfm.2007.01.008

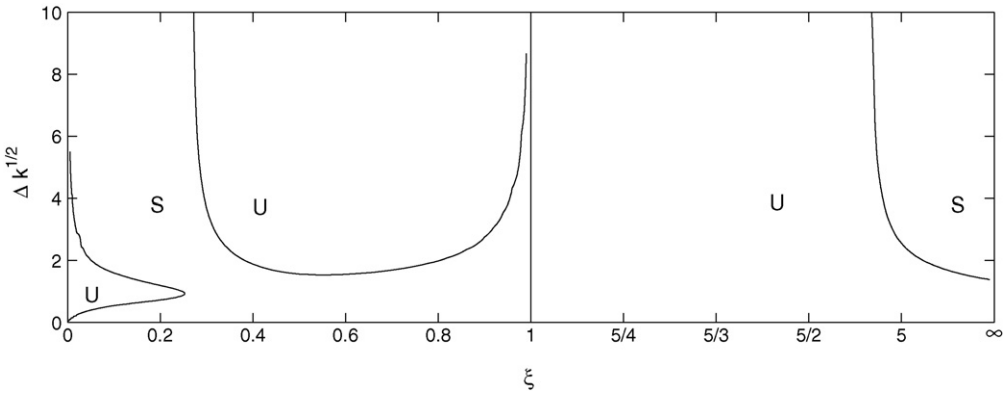

Fig. 12. Marginal stability curves for sinuous narrow-core UCM channel modes. Computations are performed for $k = 4000$. U and S denote unstable and stable regions, respectively. Note that for $\xi > 1$ the ξ-axis has been rescaled.

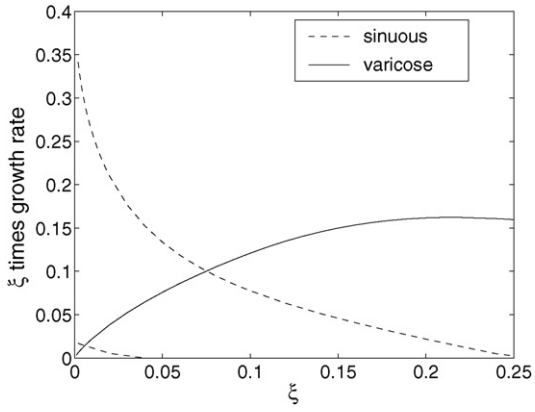

Fig. 13. UCM channel modes. Growth rate multiplied by ξ. This corresponds to the growth rate scaled by the outer fluid relaxation time. For each mode and value of ξ, Δ is chosen to maximize the growth rate.

uniformly in k. As $\beta \to 1$, one mode appears to have $\Delta \sim ck^{-1/2}$ with c growing. Another mode appears to keep approximately the same size prefactor, but its growth rate reduces.

In Fig. 18(d) we see that for $\beta = 0.99$ the marginal stability curve for which $\Delta \to \sqrt{2} - 1$ as $k \to 0$ is almost parallel to the k-axis until k is at least 100. Thus, although the corresponding wavelength is not long compared to the relaxation length scale, the long-wave result of [8,13] still applies. The reason is that as $\beta \to 1$, the elastic stress has an effect only at the interface and the fluids may otherwise be taken to be Newtonian on the length scale of the wavelength.

5. Instabilities in core-annular pipe coextrusion flow for $Wi \gg 1$

In this section we compare the stability of core-annular pipe flow with the corresponding channel flow. We consider only UCM fluids at large Wi.

For $\xi = 0.2$ and $\xi = 0.3$ we plot growth rates of axisymmetric ($m = 0$) modes in Fig. 19 as k and Δ change. The results are qualitatively similar to those seen in Fig. 6 for channel flow. When $\xi = 0.2$ we again find values of Δ for which both $k \to 0$ and $k \to \infty$ limits are stable, with an instability at an intermediate value of k, due to a narrow-core instability.

Most other results also carry over from channel flow, but there are some notable differences, particularly in the $m = 1$ cork-screw modes as described below.

5.1. Fast-flow pipe modes ($k \to \infty$)

Holding Δ fixed and increasing k corresponds to the fast-flow limit in which the relaxation length scale is large compared to the wavelength, which is itself large compared to the pipe width. In channel flow we found that the growth or decay of two-dimensional modes is determined within a boundary layer much thinner than the channel width. The curvature of the pipe is negligible over this length scale and so the same modes exist, regardless of the value of m.

For two-dimensional Couette flow [3] we found five distinct fast-flow modes. At most one is unstable, and instability occurs for $\xi_c < \xi < \xi_c^{-1}$ unless $\xi = 1$. In Fig. 20 we plot the numerically determined eigenvalues ω for pipe flow with $m = 0$ or $m = 1$, $\Delta = 0.3, k = 100$, and ξ between 0 and 1. We find all five modes expected, and they are the same for $m = 0$ and $m = 1$. However, we also find one additional mode different for $m = 0$ and $m = 1$, but always stable. For $m = 0$ the equations involving $v_\theta, a_{r\theta}$, and $a_{\theta\theta}$ decouple from the remainder, and this additional mode has $v_r = v_z = 0$ (i.e., it is a pure swirl mode) and travels with the velocity of the interface.

5.2. Narrow-core pipe modes ($\Delta \sim k^{-1/2}$, $k \to \infty$)

The narrow-core regime of Section 4 persists for pipe flow, but the curvature of the unperturbed interface remains important. We plot the stability in Figs. 21 and 22. Near $\xi = 1$, there is a quadratic minimum in the growth rate close to the marginal stability curve if $\Delta k^{1/2}$ is not small, and so the (linear) interpolation used to plot the contours is poor.

5.2.1. Axisymmetric ($m = 0$) modes

Fig. 21 shows the stability at $k = 1000$ for $m = 0$ modes. The stability boundaries are qualitatively similar to varicose channel modes as shown by a comparison of Figs. 21 and 11. For $\xi > 1$ the behaviors are practically identical. When $\xi < 1$ there are some small differences. For channel flow [Fig. 11] there is a

Please cite this article in press as: J.C. Miller, J.M. Rallison, Instability of coextruded elastic liquids at high Weissenberg number, J. Non-Newtonian Fluid Mech. (2007), doi:10.1016/j.jnnfm.2007.01.008

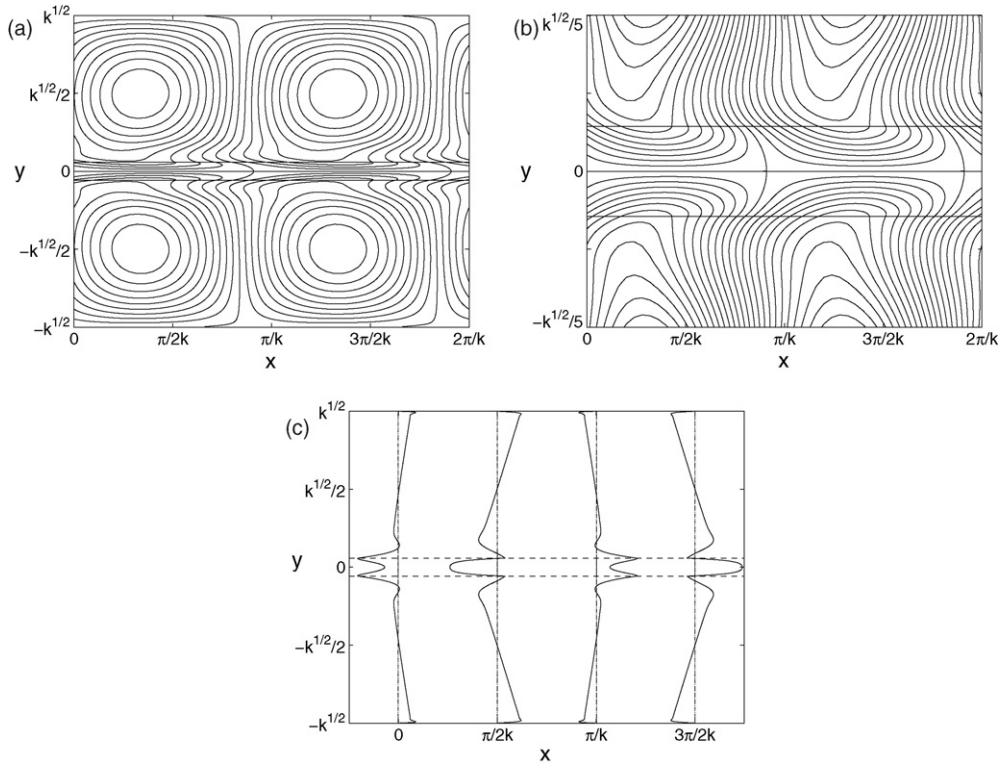

Fig. 14. UCM fluids. The perturbation flow for a varicose mode at $k = 400$ with $\xi = 0.2$ choosing $\Delta = 0.058$ to maximize the growth rate. Note that the perturbation flow fills the channel. (a) Streamlines for the varicose mode. (b) Zoom in on central boundary layer. (c) Perturbed x-velocity. The wall boundary layers are almost too small to be seen.

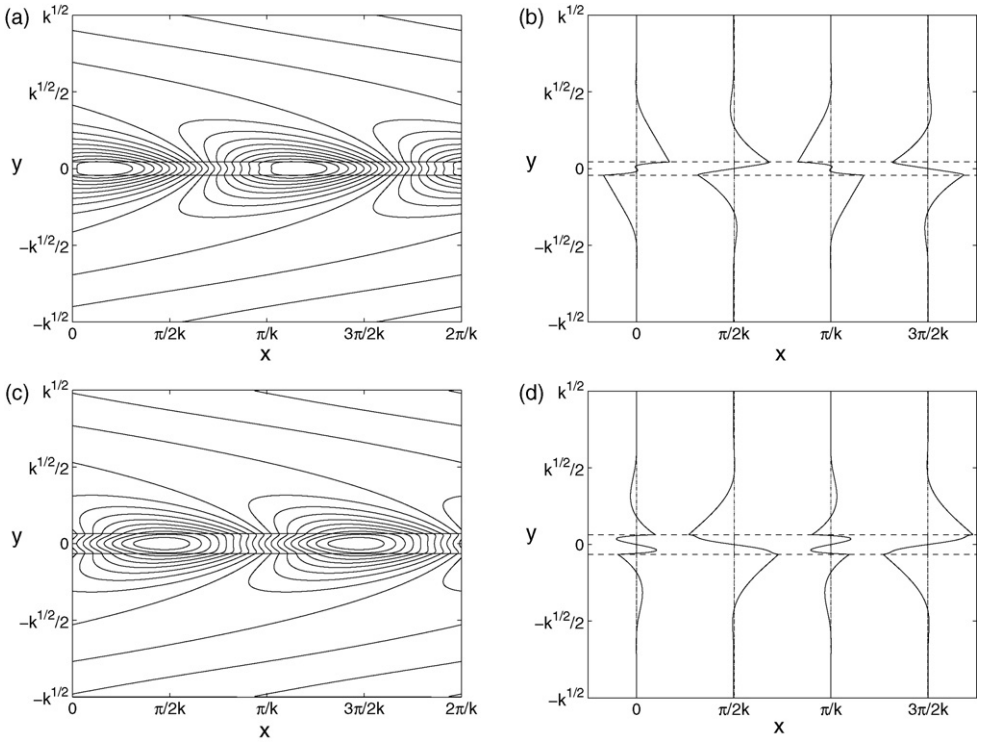

Fig. 15. The perturbation flows for UCM sinuous modes with $k = 400$ and $\xi = 0.025$. We take $\Delta = 0.043$ for the fast mode and $\Delta = 0.064$ for the slow mode, chosen to maximize each growth rate. In contrast to varicose modes, these modes decay away from the central boundary layer. For the fast mode $\omega = 418.58 + 7.66\mathrm{i}$ and for the slow mode $\omega = 395.30 + 0.0985\mathrm{i}$. (a) Streamlines for the fast sinuous mode. (b) Fast mode perturbed x-velocity. (c) Streamlines for the slow sinuous mode. (d) Slow mode perturbed x-velocity.

Please cite this article in press as: J.C. Miller, J.M. Rallison, Instability of coextruded elastic liquids at high Weissenberg number, J. Non-Newtonian Fluid Mech. (2007), doi:10.1016/j.jnnfm.2007.01.008

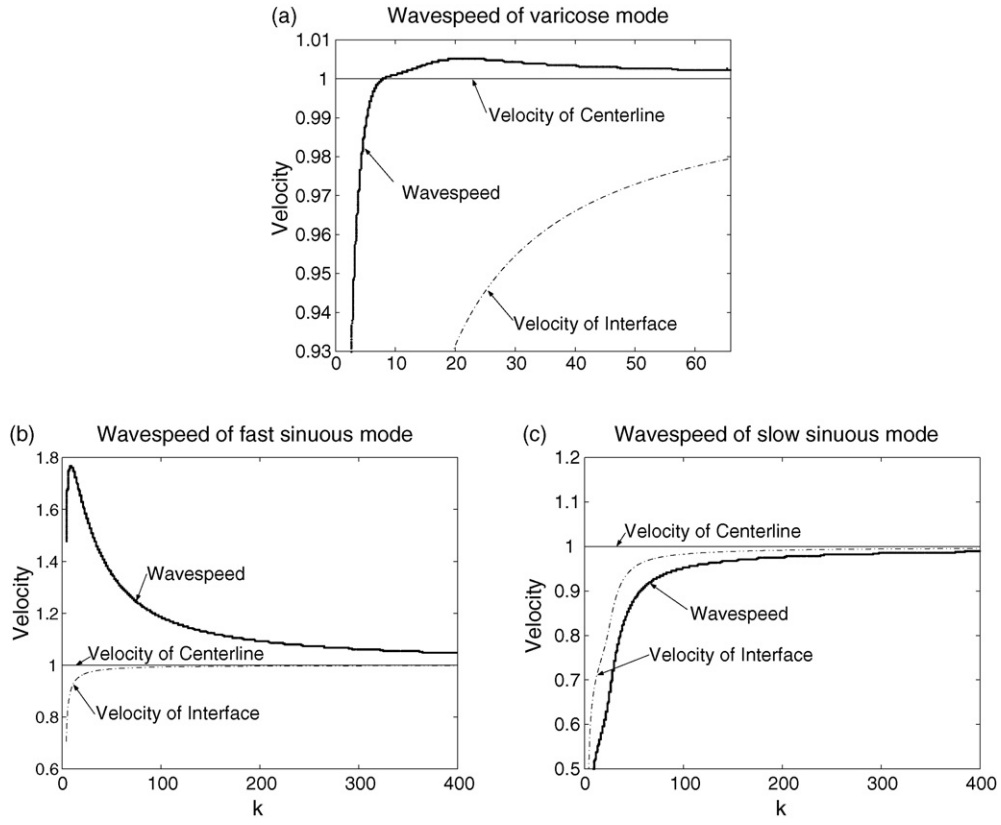

Fig. 16. UCM fluids. Wavespeed of varicose and sinuous modes compared to the velocities of the centerline and interface. For each k, Δ is chosen to give the maximum growth rate. (a) Wavespeed of varicose mode with $\xi = 0.2$. (b) Wavespeed of fast-moving sinuous mode with $\xi = 0.025$. (c) Wavespeed of slow-moving sinuous mode with $\xi = 0.025$.

small band of stability between the Couette-like fast-flow and narrow-core instabilities; in pipe flow the two regions of instability overlap. The island of stability we found in channel flow at small ξ changes qualitatively. Whereas in channel flow there is varicose instability for fixed $\Delta k^{1/2}$ as $\xi \to 0$, axisymmetric modes are stable if $\Delta k^{1/2}$ is large enough. There is a thin island of instability for axisymmetric modes.

5.2.2. *Cork-screw ($m = 1$) modes*

Fig. 22 plots the stability at $k = 1000$ for $m = 1$ modes. The qualitative behavior for $\xi > 1$ is similar to sinuous channel modes (Fig. 12), however when ξ is small, the behavior differs. At small ξ there are two sinuous narrow-core instabilities in channel flow whose growth rate scales like $1/\xi$. In $m = 1$ pipe flow, there is no corresponding instability.

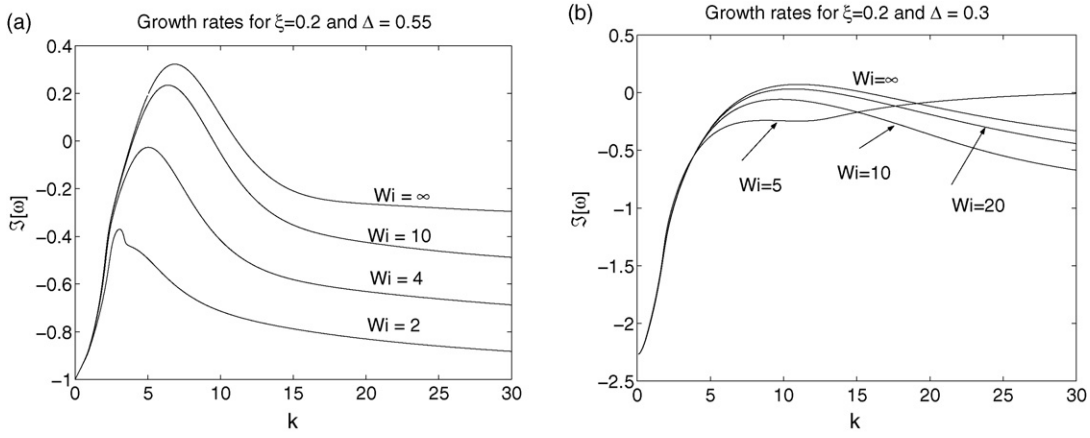

Fig. 17. UCM fluids. Convergence to the $Wi = \infty$ growth rate. As expected, convergence is faster for small k. The sinuous instability for $Wi = 5$ where $k \gg Wi$ is the wide-channel instability found by Renardy [1]. (a) Growth rate of varicose modes: $\xi = 0.2$ and $\Delta = 0.55$, with $Wi = 2$, 4, 10, and ∞. (b) Growth rate of sinuous modes: $\xi = 0.2$ and $\Delta = 0.3$ with $Wi = 5$, 10, 20, and ∞.

Please cite this article in press as: J.C. Miller, J.M. Rallison, Instability of coextruded elastic liquids at high Weissenberg number, J. Non-Newtonian Fluid Mech. (2007), doi:10.1016/j.jnnfm.2007.01.008

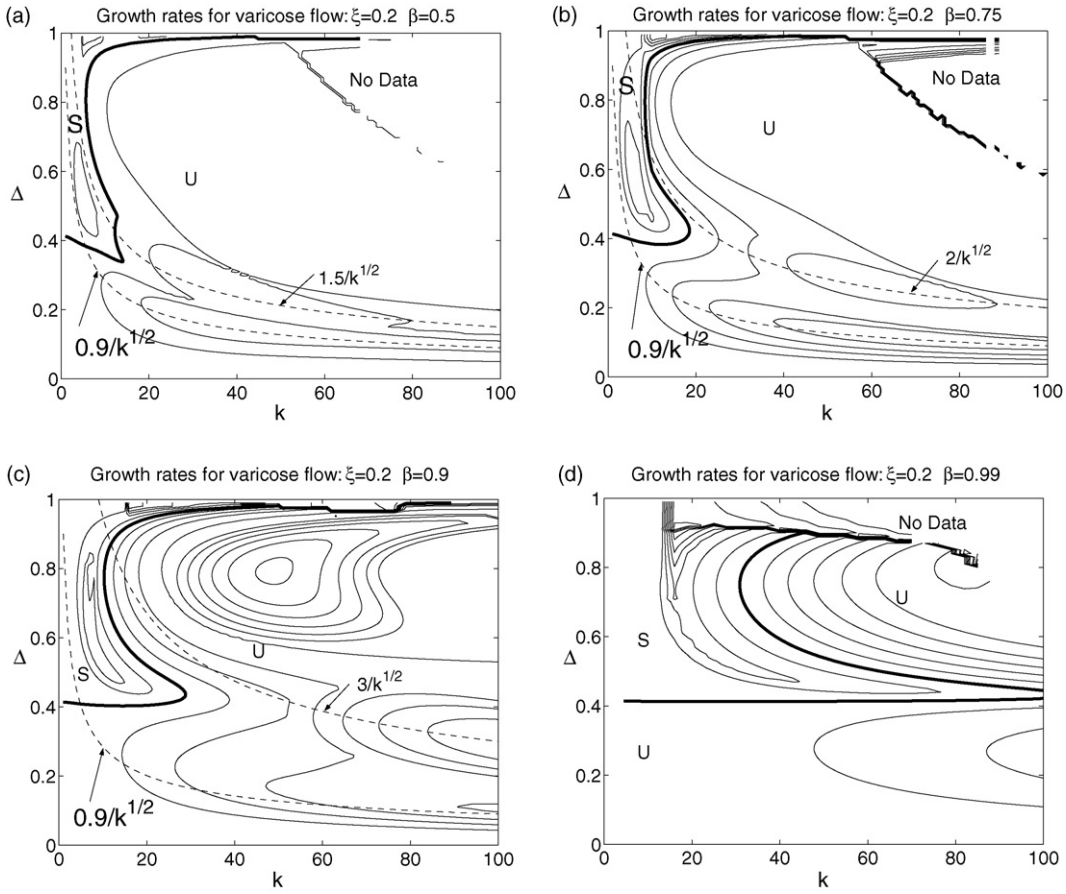

Fig. 18. Oldroyd-B fluids. Growth rates for varicose modes with $\xi = 0.2$. Compare with Fig. 6(a) for the UCM fluid. (a) $\beta = 0.5$. (b) $\beta = 0.75$. (c) $\beta = 0.9$. (d) $\beta = 0.99$.

6. Other instabilities of channel coextrusion flow

We have observed some $Wi \gg 1$ instabilities when the outer fluid layer is thin which do not fall into the long-wave, Couette-like fast-flow, or narrow-core regimes. In these cases it appears that the wall and interfacial boundary layers overlap.

6.1. UCM fluids

Fig. 23 shows a varicose instability for UCM fluids at $\xi = 0.0125$ with Δ apparently approaching 1 as $k \to \infty$. The existence of this mode has been confirmed with both shooting and spectral methods. The shooting method could not resolve the behavior for $k > 30$, and the remaining results shown use the spectral method. As k increases, the number of Chebyshev polynomials retained per variable increases (from 70 successively to 240) resulting in apparent jumps in the growth rate. The exact stability boundary should be regarded with some suspicion.

Because ξ is small, the interfacial boundary layer in the outer fluid reaches the wall. The shear rate variation across the boundary layer is small (and decreases as k grows), and so the flow near the interface is effectively Couette. However, we have performed a partial search in Couette flow with similar parameters and have not found a corresponding instability. We tentatively suggest that the variation in shear rate, though small, may play some role in the instability mechanism.

6.2. Oldroyd-B fluids

The contours in Fig. 18(c) for $\beta = 0.9, \xi = 0.2$ show a maximum of the varicose growth rate at $k \approx 50$, $\Delta \approx 0.8$. As k increases the value of Δ for the associated mode appears to approach 1, that is, the interface is close to the wall. Fig. 24 clearly shows that this instability is distinct from the Couette-like fast-flow instability. A corresponding instability has been found in Couette flow [3]. Both are unexplained.

7. Discussion

We have shown that in general the stability of large Wi coextrusion flow in a channel or a pipe is closely related to that of large Wi Couette channel flow, though the mode structure is different. However, when the interface is close to the center, the Couette analysis no longer applies and we find a new class of purely elastic interfacial instabilities for which $\Delta \sim k^{-1/2}$. These narrow-core instabilities can exist at intermediate wavenumbers when the $k \to 0$ and $k \to \infty$ limits are both stable.

Please cite this article in press as: J.C. Miller, J.M. Rallison, Instability of coextruded elastic liquids at high Weissenberg number, J. Non-Newtonian Fluid Mech. (2007), doi:10.1016/j.jnnfm.2007.01.008

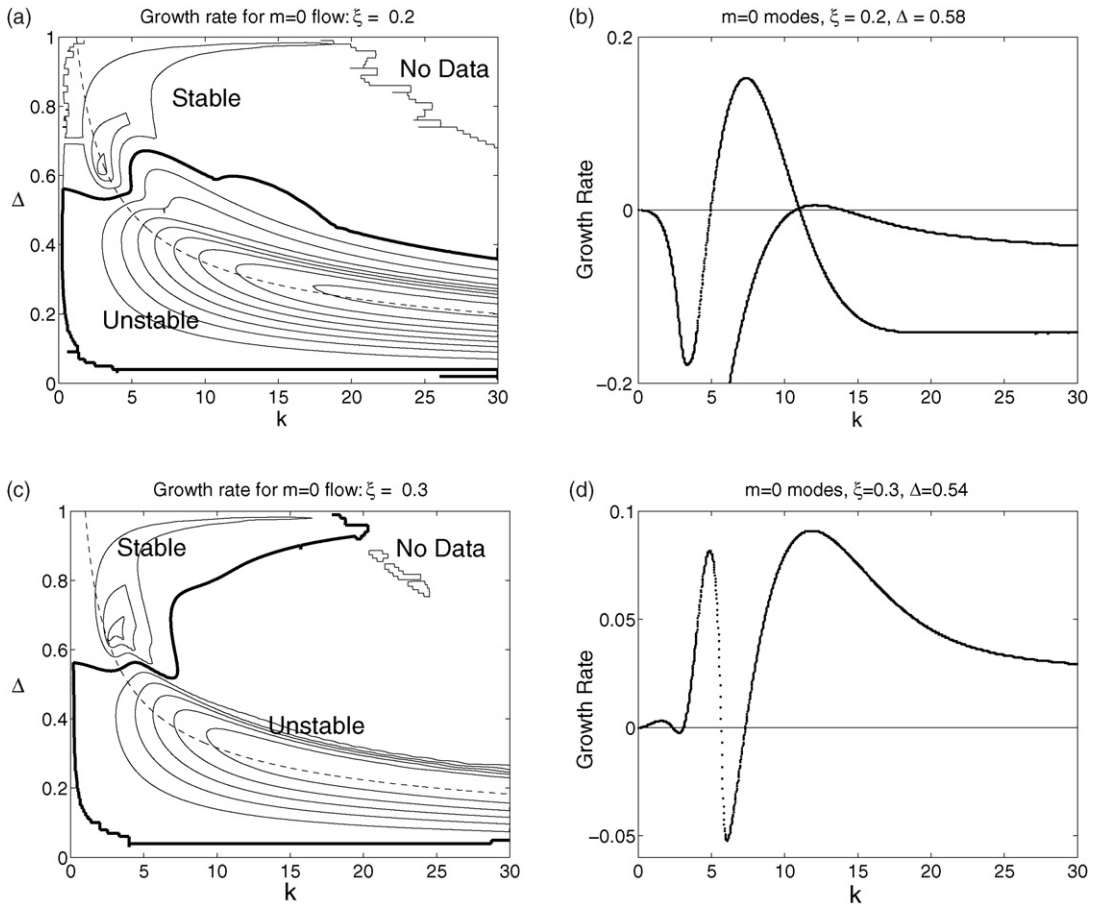

Fig. 19. Pipe flow of UCM fluids. Growth rates for $m = 0$ mode with $\xi = 0.2$ and $\xi = 0.3$. Dashed lines in (a) and (b) show constant $\Delta k^{1/2}$. (a) Growth rate of most dangerous axisymmetric mode, $\xi = 0.2 < \xi_c$. (b) Growth rates of the two unstable axisymmetric modes, $\xi = 0.2$, $\Delta = 0.58$. (c) Growth rate of most dangerous axisymmetric mode, $\xi = 0.3 > \xi_c$. (d) Growth rate of the single unstable axisymmetric mode, $\xi = 0.3$, $\Delta = 0.54$.

Fast-flow modes – for which the distance travelled by a fluid particle in a relaxation time is large compared to both the wavelength and the channel width – can be divided into Couette-like fast-flow modes and narrow-core modes. The former depend on a boundary layer at the interface with a thickness proportional to the inverse shear rate. Provided that the shear rate is effectively constant over the boundary layer width, the stability properties are identical to those of the fast-flow modes found in Couette flow. Close to the center, however, the inverse shear rate becomes large, while U'/U'', the distance over which the shear rate changes becomes small. The inverse shear rate is not effectively constant over the boundary layer width, and the narrow-core modes are found.

Through a parameter continuation argument we can conclude the *existence* of instabilities in narrow-core modes without any recourse to calculations. When $\xi = 1$ the growth rate of the interfacial mode must be zero because the fluids are identical. Generically there exists stability and instability on alternate sides of $\xi = 1$ because the derivative of the growth rate with respect to ξ is nonzero (unbounded Couette flow is not generic owing to a symmetry which is absent in coextrusion flow). The same argument shows that if there are just two layers in the channel with a single interface sufficiently close to the center there must be narrow-core instabilities for some value of ξ close to one (although the name is a misnomer in this case since there is no core fluid).

We can extend these ideas to any constitutive model which predicts an interfacial boundary layer thickness for a perturbation flow which is inversely proportional to the shear rate in Couette flow. Whenever the interface is close to the centerline, the boundary layer structure must change because the local inverse shear rate diverges. The growth rate must cross zero when the two fluids are identical, and so we must have narrow-core instabilities for some parameter values when the interface is close to the center.

This argument suggests that the phenomenon of narrow-core instability is robust for elastic liquids, but we are not aware of experimental evidence to support our analysis.

We observe that the narrow-core instability may persist to relatively large values of the Reynolds number, as long as the flow remains laminar. The local Reynolds number (based on the relative velocity and distance between the interface and centerline) will be small even if the global Reynolds number is not. Consequently inertia should be unimportant in the region that determines the growth rate.

When the core is narrow in pipe flow, the curvature of the interface is not negligible and so it affects the stability properties, qualitatively changing the narrow-core results. This is

Please cite this article in press as: J.C. Miller, J.M. Rallison, Instability of coextruded elastic liquids at high Weissenberg number, J. Non-Newtonian Fluid Mech. (2007), doi:10.1016/j.jnnfm.2007.01.008

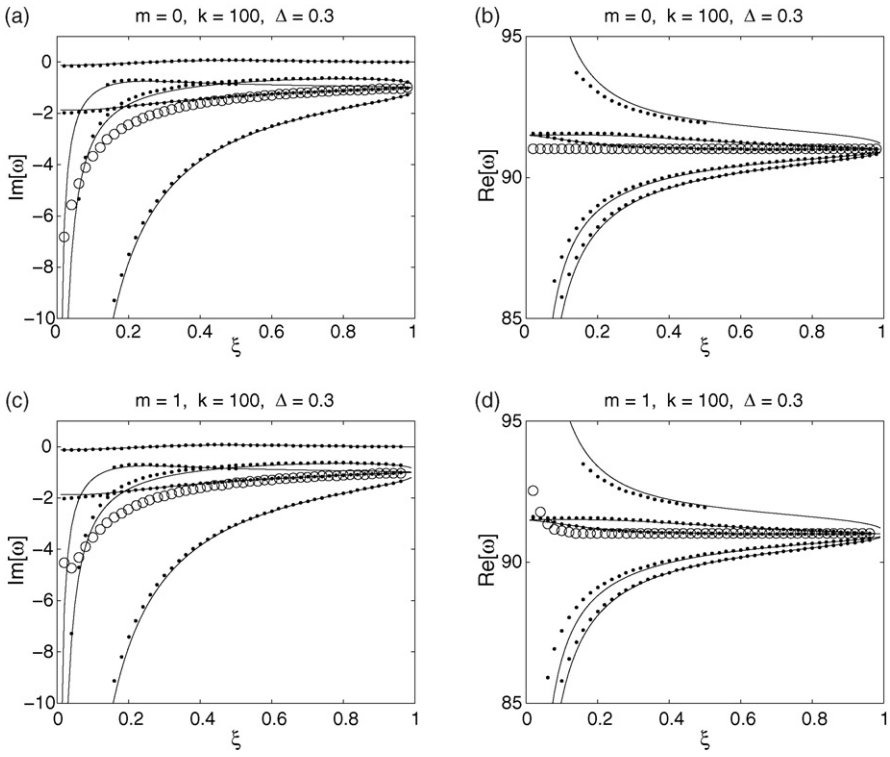

Fig. 20. Pipe flow of UCM fluids. Dots show modes for $k = 100$, $\Delta = 0.3$. The solid lines are $k \to \infty$ predictions from 2D Couette flow [3]. An additional stable mode not predicted by [3] is depicted by circles. One mode could be calculated only for a limited range of ξ owing to interference of the insufficiently resolved continuous spectrum [8]. (a) Imaginary part of ω for $m = 0$ modes. (b) Real part of ω for $m = 0$ modes. (c) Imaginary part of ω for $m = 1$ modes. (d) Real part of ω for $m = 1$ modes.

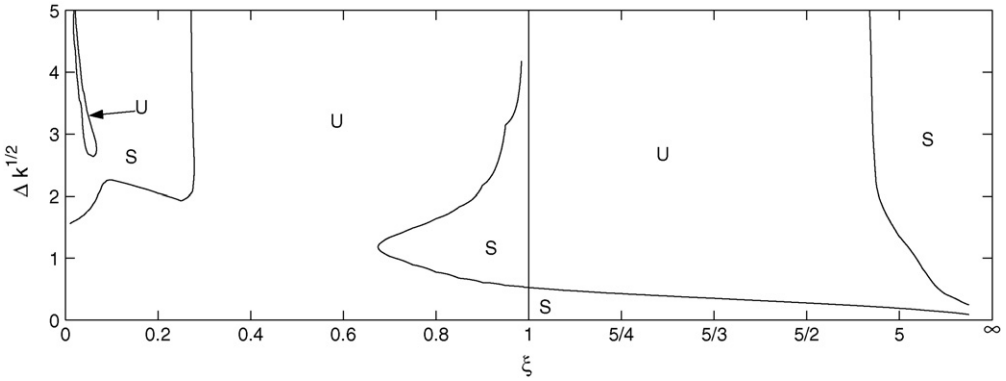

Fig. 21. Pipe flow of UCM fluids. Marginal stability curves of $m = 0$ modes in $(\xi, \Delta k^{1/2})$ space for $k = 1000$. U and S denote unstable and stable regions, respectively. The stability boundary for $0.9 < \xi < 1$, $\Delta k^{1/2} > 3$ is affected by low resolution. Compare with Fig. 11 for varicose channel modes.

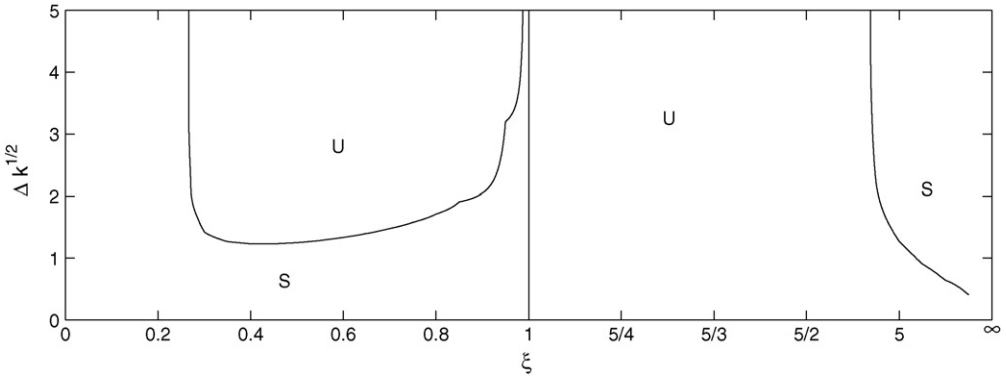

Fig. 22. Pipe flow of UCM fluids. Marginal stability curves of $m = 1$ modes in $(\xi, \Delta k^{1/2})$ space for $k = 1000$. U and S denote unstable and stable regions, respectively. Compare with Fig. 12 for sinuous channel modes. As in Fig. 21 the marginal stability curve for $0.8 < \xi < 1$ is affected by poor resolution.

Please cite this article in press as: J.C. Miller, J.M. Rallison, Instability of coextruded elastic liquids at high Weissenberg number, J. Non-Newtonian Fluid Mech. (2007), doi:10.1016/j.jnnfm.2007.01.008

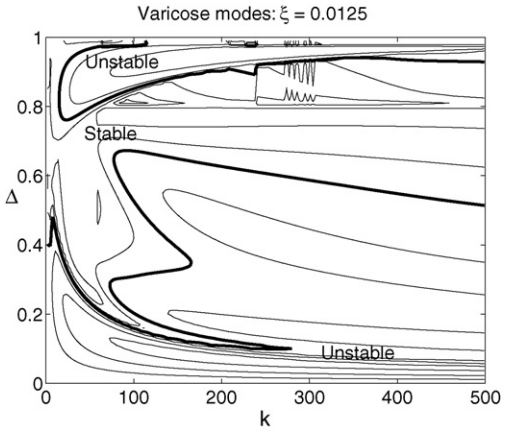

Fig. 23. Channel flow of UCM fluids. An unstable varicose mode appears at large Δ and small ξ. This instability does not fall into any category previously identified.

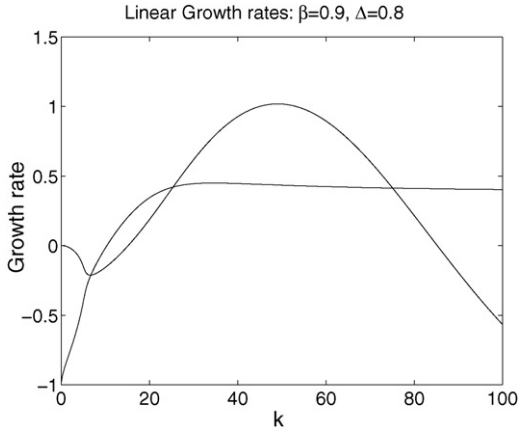

Fig. 24. Channel flow of an Oldroyd-B fluid. Varicose growth rates for $\xi = 0.2$, $\beta = 0.9$, and $\Delta = 0.8$. In addition to the Couette-like fast-flow mode having constant growth rate as $k \to \infty$, there is an additional instability which exists for moderate k.

particularly significant at small ξ where there is no instability for cork-screw modes, while in sinuous channel modes there is an instability with large growth rate.

In addition to the narrow-core instability, we have found some other purely elastic instabilities when the interface is close to the channel walls. These instabilities are not explained by the analysis presented here, but occur for small values of ξ in circumstances where the interfacial boundary layer in the outer fluid overlaps the wall boundary layer.

The results of this paper suggest a wealth of possible future weakly nonlinear study. A method for constructing a weakly nonlinear analysis of flows with interfaces is given by Renardy and Renardy [14]. It is necessary to consider the moderate k instability as well as the $k = 0$ mode. Fig. 8 shows that two separate moderate k modes are important for some parameters.

Acknowledgments

Some of this work was done while JCM visited the Institute of Theoretical Geophysics, University of Cambridge. JCM was supported under a National Science Foundation Graduate Research Fellowship and by the Department of Energy at LANL under Contract No. DE-AC52-06NA25396 and the DOE Office of ASCR program in Applied Mathematical Sciences.

Appendix A. Linear perturbation equations and non-dimensionalization

A.1. Linear perturbation equations for channel flow

We now derive the linear perturbation equations for channel flow. We consider a small perturbation to the base state, denoting perturbation quantities by lowercase letters, with solutions proportional to $\exp(\mathrm{i}kx - \mathrm{i}\omega t)$.

We use the symbol 'D' to denote a derivative with respect to y. We introduce a streamfunction ψ so that $\boldsymbol{u} = (\mathrm{D}\psi, -\mathrm{i}k\psi)$, satisfying incompressibility automatically. Taking the curl of the momentum equation yields the perturbed vorticity equation

$$\beta(\mathrm{D}^2 - k^2)^2\psi + \frac{1-\beta}{\tau}[(\mathrm{D}^2 + k^2)a_{12} + \mathrm{i}k\mathrm{D}(a_{11} - a_{22})] = 0. \tag{A.1}$$

The constitutive Eq. (3) gives

$$\begin{aligned} \alpha a_{11} &= 2U' a_{12} + 2(1 + 2\tau^2 U'^2)\mathrm{i}k\mathrm{D}\psi + 2\tau U'\mathrm{D}^2\psi \\ &\quad + 4\tau^2 U' U''\mathrm{i}k\psi, \\ \alpha a_{12} &= U' a_{22} + \mathrm{D}^2\psi + (1 + 2\tau^2 U'^2)k^2\psi + \mathrm{i}k\tau U''\psi, \\ \alpha a_{22} &= 2k^2\tau U'\psi - 2\mathrm{i}k\mathrm{D}\psi, \end{aligned} \tag{A.2}$$

where $\alpha = -\mathrm{i}\omega + \mathrm{i}kU + 1/\tau$.

The no-slip boundary condition at $y = L$ gives

$$\psi(L) = \mathrm{D}\psi(L) = 0. \tag{A.3}$$

If the perturbation is sinuous, ψ is an even function while ψ is odd if the perturbation is varicose and thus

$$\mathrm{D}\psi(0) = \mathrm{D}^3\psi(0) = 0 \qquad \text{(sinuous)}, \tag{A.4}$$

$$\psi(0) = \mathrm{D}^2\psi(0) = 0 \qquad \text{(varicose)}. \tag{A.5}$$

The interface is a material surface, so at the interface

$$(-\mathrm{i}\omega + \mathrm{i}kU)\delta = -\mathrm{i}k\psi \tag{A.6}$$

where δ measures interfacial perturbation and U and ψ are evaluated at the interface $y = \Delta L$. The conditions at the interface give

$$[\![\psi]\!]_{\Delta L} = 0, \tag{A.7}$$

$$[\![\mathrm{D}\psi]\!]_{\Delta L} = 0, \tag{A.8}$$

$$\left[\!\!\left[\beta\mathrm{D}^2\psi - 2\mathrm{i}kU'^2\tau(1-\beta)\delta + \frac{1-\beta}{\tau}a_{12}\right]\!\!\right]_{\Delta L} = 0, \tag{A.9}$$

$$\left[\!\!\left[\beta\frac{\mathrm{i}}{k}\mathrm{D}^3\psi + \frac{1-\beta}{\tau}\left(\frac{\mathrm{i}}{k}\mathrm{D}a_{12} - a_{11} + a_{22}\right)\right]\!\!\right]_{\Delta L} = 0. \tag{A.10}$$

Please cite this article in press as: J.C. Miller, J.M. Rallison, Instability of coextruded elastic liquids at high Weissenberg number, J. Non-Newtonian Fluid Mech. (2007), doi:10.1016/j.jnnfm.2007.01.008

A.2. Linear perturbation equations for pipe flow

We now derive the linear perturbation equations for pipe flow, following a similar non-dimensionalization to that of channel flow (Section 2.2). We use (r, θ, z) variables with D now denoting differentiation with respect to r. We look for linear modes proportional to $\exp(\mathrm{i}kz + \mathrm{i}m\theta - \mathrm{i}\omega t)$. If $m = 0$ we have axisymmetric modes, analogous to varicose modes in a channel, and if $m = 1$ we have cork-screw or helical modes, analogous to sinuous modes. We have not considered other values of m.

The incompressibility condition becomes

$$\frac{1}{r}\mathrm{D}(rv_r) + \frac{\mathrm{i}m}{r}v_\theta + \mathrm{i}v_z = 0, \tag{A.11}$$

where $\boldsymbol{u} = (v_r, v_\theta, v_z)$. The r-, θ-, and z-components of the momentum equation become

$$\mathrm{D}\left(-\frac{Wi^2}{k}p + \frac{a_{rr}}{\tau}\right) + \frac{1}{r}\frac{a_{rr}}{\tau} + \mathrm{i}m\frac{a_{r\theta}}{\tau} + \mathrm{i}\frac{a_{rz}}{\tau} - \frac{1}{r}\frac{a_{\theta\theta}}{\tau} = 0, \tag{A.12}$$

$$\frac{1}{r^2}\mathrm{D}\left(r^2\frac{a_{r\theta}}{\tau}\right) + \frac{\mathrm{i}m}{r}\left(-\frac{Wi^2}{k}p + \frac{a_{\theta\theta}}{\tau}\right) + \mathrm{i}\frac{a_{\theta z}}{\tau} = 0, \tag{A.13}$$

$$\frac{1}{r}\mathrm{D}\left(r\frac{a_{rz}}{\tau}\right) + \frac{\mathrm{i}m}{r}\frac{a_{\theta z}}{\tau} + \mathrm{i}\left(-p + \frac{a_{zz}}{\tau}\right) = 0. \tag{A.14}$$

The constitutive equations become

$$\alpha a_{rr} = 2\mathrm{D}v_r - 4\mathrm{i}r\tau v_r, \tag{A.15}$$

$$\alpha a_{r\theta} = \frac{\mathrm{i}m}{r}v_r + \mathrm{D}v_\theta - \frac{v_\theta}{r} - 2\mathrm{i}\tau r v_\theta, \tag{A.16}$$

$$\alpha a_{\theta\theta} = \frac{2}{r}(\mathrm{i}m v_\theta + v_r), \tag{A.17}$$

$$\alpha a_{rz} = -2ra_{rr} - 2\tau r\mathrm{D}v_r + 8\mathrm{i}\tau^2 r^2 v_r + \mathrm{D}v_z - 2\mathrm{i}\tau r v_z + 2\tau v_r + \frac{k}{Wi^2}\mathrm{i}v_r, \tag{A.18}$$

$$\alpha a_{\theta z} = -2ra_{r\theta} - 2\tau r\mathrm{D}v_\theta + 8\mathrm{i}\tau^2 r^2 v_\theta + \frac{\mathrm{i}m}{r}v_z + 2\tau v_\theta + \frac{k}{Wi^2}\mathrm{i}v_\theta, \tag{A.19}$$

$$\alpha a_{zz} = -4ra_{rz} - 4\tau r\mathrm{D}v_z + 16\mathrm{i}\tau^2 r^2 v_z - 16\tau^2 r v_r + \frac{k}{Wi^2}2\mathrm{i}v_z, \tag{A.20}$$

where $\alpha = -\mathrm{i}\omega + \mathrm{i}k - \mathrm{i}r^2 + 1/\tau$. At the interface we have continuity of velocity

$$[\![v_r]\!]_{\Delta k^{1/2}} = [\![v_\theta]\!]_{\Delta k^{1/2}} = [\![v_z]\!]_{\Delta k^{1/2}} = 0, \tag{A.21}$$

and continuity of surface traction

$$\left[\!\!\left[-p + \frac{k}{Wi^2}\frac{a_{rr}}{\tau}\right]\!\!\right]_{\Delta k^{1/2}} = \left[\!\!\left[\frac{a_{r\theta}}{\tau}\right]\!\!\right]_{\Delta k^{1/2}} = \left[\!\!\left[-8\mathrm{i}\tau\delta r^2 + \frac{a_{rz}}{\tau}\right]\!\!\right]_{\Delta k^{1/2}} = 0 \tag{A.22}$$

Note that the surface traction conditions do not involve m. If the constitutive equation had a nonzero second normal stress difference N_2, then there would be m dependence. The perturbed interface location is given by the kinematic condition

$$(-\mathrm{i}\omega + \mathrm{i}k - \mathrm{i}r^2)\delta = v_r. \tag{A.23}$$

A.2.1. Boundary conditions

At the walls $r = k^{1/2}$ no-slip gives

$$v_r = 0, \quad v_\theta = 0, \quad v_z = 0. \tag{A.24}$$

The boundary conditions at the origin differ for $m = 0$ and $m = 1$ [15]. For $m = 0$, incompressibility (A.11) implies

$$v_r(0) = 0 \quad (m = 0). \tag{A.25}$$

Because the streamwise perturbation velocity is smooth at $r = 0$, we find

$$\mathrm{D}v_z(0) = 0 \quad (m = 0). \tag{A.26}$$

This condition can also be derived by assuming that the solution is regular and matching powers of r as $r \to 0$. We assume also that

$$v_\theta(0) = 0 \quad (m = 0). \tag{A.27}$$

For $m = 1$, the incompressibility condition (A.11) gives

$$\frac{\partial v_r}{\partial r} = -\frac{v_r + \mathrm{i}v_\theta}{r} - \mathrm{i}v_z$$

and so

$$v_r(0) = -\mathrm{i}v_\theta(0) \quad (m = 1). \tag{A.28}$$

Since both v_z and p represent physical variables which cannot depend on θ at $r = 0$, we can further conclude

$$v_z(0) = p(0) = 0 \quad (m = 1). \tag{A.29}$$

As for channel flow, if $k/Wi^2 \ll 1$ we can eliminate k from the problem except for specifying the location of the interface and the cylinder wall. Assuming that the wall is far enough from the interface to not affect the growth rate, we can use the substitution $\Omega = \omega - k$ to show that k and Δ appear only in the combination $\Delta k^{1/2}$.

References

[1] Y. Renardy, Stability of the interface in two-layer Couette flow of upper convected Maxwell liquids, J. Non-Newtonian Fluid Mech. 28 (1988) 99–115.
[2] K. Chen, D.D. Joseph, Elastic short wave instability in extrusion flows of viscoelastic liquids, J. Non-Newtonian Fluid Mech. 42 (1992) 189–211.
[3] J.C. Miller, J.M. Rallison, Interfacial instability between sheared elastic liquids in a channel, submitted for publication.
[4] P. Laure, H.L. Meur, Y. Demay, J.C. Saut, S. Scotto, Linear stability of multilayer plane Poiseuille flows of Oldroyd-B fluids, J. Non-Newtonian Fluid Mech. 71 (1997) 1–23.
[5] S. Scotto, P. Laure, Linear stability of three-layer Poiseuille flow for Oldroyd-B fluids, J. Non-Newtonian Fluid Mech. 83 (1999) 71–92.

Please cite this article in press as: J.C. Miller, J.M. Rallison, Instability of coextruded elastic liquids at high Weissenberg number, J. Non-Newtonian Fluid Mech. (2007), doi:10.1016/j.jnnfm.2007.01.008

[6] K.-P. Chen, Interfacial instability due to elastic stratification in concentric coextrusion of two viscoelastic fluids, J. Non-Newtonian Fluid Mech. 40 (1991) 155–175.
[7] E.J. Hinch, O.J. Harris, J.M. Rallison, The instability mechanism for two elastic liquids being co-extruded, J. Non-Newtonian Fluid Mech. 43 (1992) 311–324.
[8] H.J. Wilson, Shear flow instabilities in viscoelastic fluids, Ph.D. Thesis, Cambridge University, Cambridge, United Kingdom, 1998.
[9] H.J. Wilson, J.M. Rallison, Short wave instability of co-extruded elastic liquids with matched viscosities, J. Non-Newtonian Fluid Mech. 72 (1997) 237–251.
[10] H.J. Wilson, J.M. Rallison, Instability of channel flow of a shear-thinning White–Metzner fluid, J. Non-Newtonian Fluid Mech. 87 (1999) 75–96.
[11] H.J. Wilson, M. Renardy, Y. Renardy, Structure of the spectrum in zero Reynolds number shear flow of the UCM and Oldroyd-B liquids, J. Non-Newtonian Fluid Mech. 80 (1999) 251–268.
[12] J.C. Miller, Shear flow instabilities in viscoelastic fluids, Ph.D. Thesis, Cambridge University, 2005.
[13] H.K. Ganpule, B. Khomami, A theoretical investigation of interfacial instabilities in the three layer superposed channel flow of viscoelastic fluids, J. Non-Newtonian Fluid Mech. 79 (1998) 315–360.
[14] M. Renardy, Y. Renardy, Derivation of amplitude equations and analysis of sideband instabilities in two-layer flows, Phys. Fluids A 5 (1993) 2738–2762.
[15] P. Luigi, K.-P. Chen, D.D. Joseph, Lubricated pipelining: stability of core-annular flow, J. Fluid Mech. 201 (1989) 323–356.

Please cite this article in press as: J.C. Miller, J.M. Rallison, Instability of coextruded elastic liquids at high Weissenberg number, J. Non-Newtonian Fluid Mech. (2007), doi:10.1016/j.jnnfm.2007.01.008